CHALMERS

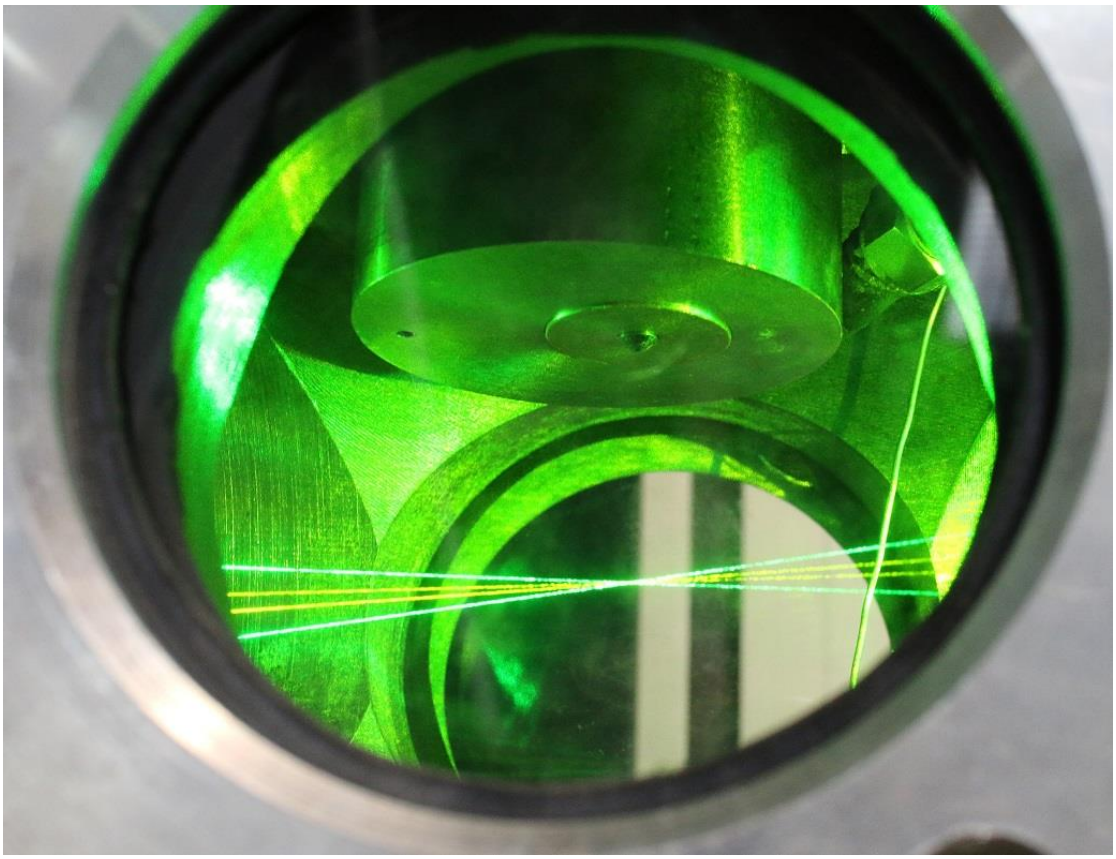

Characterization of GDI fuel sprays using Phase Doppler Interferometry

Master's Thesis in the Master Degree Programme, Automotive Engineering

Nikolaos Dimitrakopoulos

Department of Applied Mechanics
Division of Combustion

CHALMERS UNIVERSITY OF TECHNOLOGY
Göteborg, Sweden 2014
Master's thesis 2014:08

MASTER'S THESIS IN AUTOMOTIVE ENGINEERING

Characterization of GDI fuel sprays using Phase Doppler Interferometry

Nikolaos Dimitrakopoulos

Department of Applied Mechanics
Division of Combustion

CHALMERS UNIVERSITY OF TECHNOLOGY
Göteborg, Sweden 2014

Characterization of GDI fuel sprays using Phase Doppler Interferometry

Nikolaos Dimitrakopoulos

© Nikolaos Dimitrakopoulos,2014

Master's Thesis 2014:08
ISSN 1652-8557
Department of Applied Mechanics
Division of Combustion
Chalmers University of Technology
SE-412 96 Göteborg
Sweden
Telephone: + 46 (0)31-772 1000

Department of Applied Mechanics
Göteborg, Sweden 2014

Abstract

Characterization of GDI fuel sprays using Phase Doppler Interferometry
Master's Thesis in the *Master's Degree Programme, Automotive Engineering*
Nikolaos Dimitrakopoulos
Department of Applied Mechanics
Division of Combustion
Chalmers University of Technology

One of the main factors that determine the combustion efficiency of an internal combustion engine and as a result the output power as well as the exhaust gas composition is the degree of mixing between the intake air and the fuel. In order to improve the air/fuel mixing the automotive industry has shifted the last five years from the port fuel injection strategies to the newer direct fuel injection which also yields more advantages. In this strategy one of the most crucial components is the fuel injector, which has to be able to deliver precise quantity of fuel, combined with excellent atomization properties that must behave according to specifications throughout different modes of operation.

In this thesis a new experimental fuel injector was provided to the Combustion division of Applied Mechanics and was evaluated in terms of spray characteristics. The most important of these are the fuel droplet diameter which is quantified by the D10 and D32 values and the droplet velocity. The droplets should have a relative small diameter, measured in μm, in order to be able to evaporate properly and fast and they should have a velocity that allows them to reach into the combustion chamber without impinging to the piston and the liner because that causes high unburned hydrocarbon emissions.

The method that was used to evaluate the performance of the injector is called Phase Doppler Anemometry. It is an optical, non-intrusive, single point, measuring method that uses a small control volume that is created by a laser source to measure accurately both velocity and diameter at the same time. Three different groups of measurements were performed. In the first the influence of the injection pressure on the velocity and the droplet diameter was evaluated. The pressure was varied from 25bar up to 200bar. In the second the influence of different injection durations while keeping constant pressure were examined again in terms of velocity and droplet diameter and in the final group the ability of the injector to perform double injection and whether that has an effect on velocities and droplet diameters.

The results showed a significant reduction in droplet diameter with the increase of the fuel pressure starting from 16,7μm at 25bar and reaching 11,7μm at 200bar while the velocities start from 19,5m/s and reach 55m/s. The different injection duration shows little influence on both the diameters and the velocities and the same can be said for the double injection. The double injection is possible and the droplet diameters as well as the velocity vary very little compared to the single injection.

Key words: phase doppler interferometry, pda, gasoline direct injection, gdi, D32, sauter mean diameter, sprays

Acknowledgements

With this master thesis project I completed my studies in the Department Applied Mechanics, Division of Combustion, of Chalmers University of Technology. I want to acknowledge the people who supported me and encouraged me in my studies during these years.

I would like to express my sincere gratitude to my project supervisor Petter Dahlander for all the support and guidance he offered me during my master thesis. I would like to thank all the people in the department that helped me during this time, especially Eugenio De Benito. Without his help and guidance I would not learn to use and operate the Phase Doppler System in such a short time.

Also many thanks to my classmates for the help and long discussions we had almost every day at the department during this period that helped me with the present work.

Table of Contents

1 Introduction

1.1 Background

One of the biggest environmental challenges of our time is the constant increase in greenhouse gases and harmful emissions as well as the depletion of fossil fuel resources. The transportation sector is one of the major consumers of oil products and as a result even a minor decrease in fuel consumption can produce big benefits. In order to reduce the fuel consumption and the exhaust emissions the engines must improve and become more efficient.

One of the major improvements for gasoline engines was the introduction of direct fuel injection, which in theory can improve the thermodynamic efficiency. Still as a new technology, direct injection is far from performing optimally. One major component that has a great impact on the performance of a direct injection system is the fuel injector and as a result many different implementations have been suggested.

1.2 Problem definition

When an engine operates with direct injection, different injection modes are available, with the most common being the stratified and homogeneous operation. Both modes pose different challenges for the injector, which must perform optimally under these conditions. During stratified operation a small volume of homogeneous mixture must be created around the spark plug in order for the combustion to be stable while the rest of the cylinder is filled with air or exhaust gases. The injector must be able to operate like that without wetting the cylinder walls or the piston crown with fuel which causes hydrocarbon and carbon monoxide emissions. During homogeneous operation the injector must be able to produce low diameter fuel droplets at reasonable injection velocity in order to mix completely with the air prior to ignition.

Since operating optimally at both operating modes is difficult, different systems have developed during the years of commercial application of direct injection, which still continue to evolve. As a result the behavior of each system and the injector as a specific component is difficult to predict and therefore modeled. If it can become easier for the injector spray to be modeled accurately, CFD simulations can lead to better results for the whole combustion process in an engine.

1.3 Purpose and aim

A new gasoline fuel injector, which is designed for direct injection engines, was delivered to the division of combustion, department of applied mechanics. The only available information regarding the injector is that is a multi-hole solenoid operated injector, designed for injection pressures of up to 200bar.

Two of the most important characteristics of a fuel injector are the spray velocity and the droplet diameters. The aim of this thesis is to try and evaluate how the injector performs, regarding these terms under different injection pressures, injection durations as well as if it possible to operate with multiple injections and what are the results of this. All the measurements will be performed with the use of an optical measurement technique, called Phase Doppler Interferometry. The results will be analyzed with the use of Matlab.

1.4 Our scope and limitations

Although the evaluation of injector sprays velocity and droplet distribution is an important parameter in order to quantify the performance of an injector, more testing is required to estimate the full potential of the injector. An extension to the ambient temperature testing that was performed for this thesis, is the high temperature testing, both for the fuel and the air inside the spray chamber. Furthermore more optical measurements must be made in order to evaluate the spray shape and other important factors such as the penetration length and the liquid-vapor phase of the fuel during injection. Finally an in-engine test must be performed so as to have better visualization during actual operation.

While all these measurements are important, the focus of this thesis is on the fundamental aspects of the injector operation and only focuses on the velocity and droplet diameters under ambient conditions.

2 Methodology – System description

2.1 Phase Doppler Anemometry System & Laser source

The phase Doppler system that was used throughout the measurements was a 2D TSI Phase Doppler Particle Analyzer. It has the ability to measure velocity components of two axes, vertical and horizontal as well as the droplet diameters. In order to operate properly and move freely both the transmitter and the receiver are place on a traverse system that can move in all three dimensions. The transmitter has a focal length of 250mm and beam separation of 40mm, at the end of the transmitter with the use of an internal beam expander. The laser light to the transmitter is produced from an Innova 90 laser system that is capable of producing laser light of 488nm (blue) and 514,5nm (green) with a maximum power of up to 5W. The transmitter is connected to the laser source with the use of specialized optical fibers. The receiver has a focal length of 350mm and the signals are processed by the TSI FSA-4000 processor and are visualized with the use of the Flowsizer software.

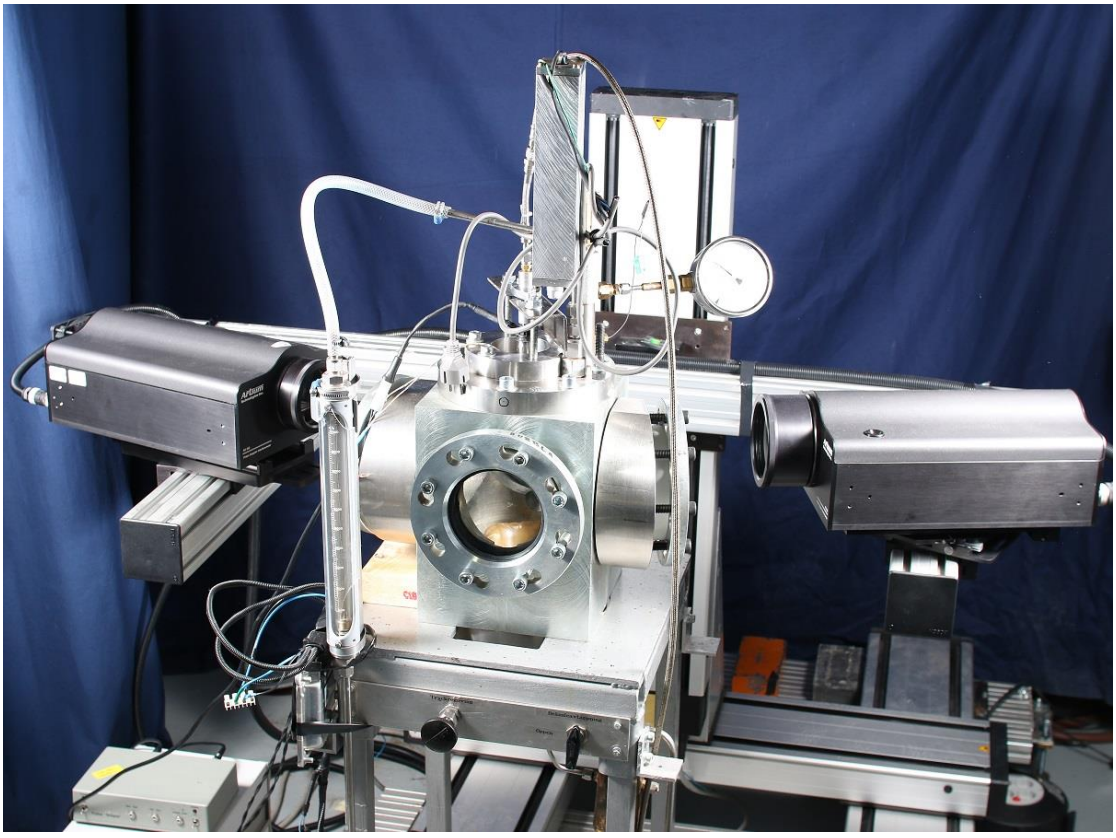

Figure 1: Phase Doppler System aligned to the spray chamber

Figure 2: FSA 4000 Processor

2.2 Spray Chamber

All of the measurements take place in the low pressure/low temperature spray chamber. The spray chamber is designed for spray studies with maximum pressure of up to 6 bar but can also operate at pressures of 0,5 bar (vacuum). The temperature of air as well as the temperature of the injector to be tested and as a result the temperature of the fuel can be controlled with the use of heating elements and can be varied from ambient temperature up to 90^{o}C. The actual chamber has a cubical shape with four large windows of XX mm diameter on each side, allowing good optical access and positioning of the measuring equipment, in this case the Phase Doppler system. On the top of the spray chamber there is an opening for a custom made external injector mounting, which is manufactured to the exact dimensions of the injector and keeps the injector in a vertical position inside the spray chamber.

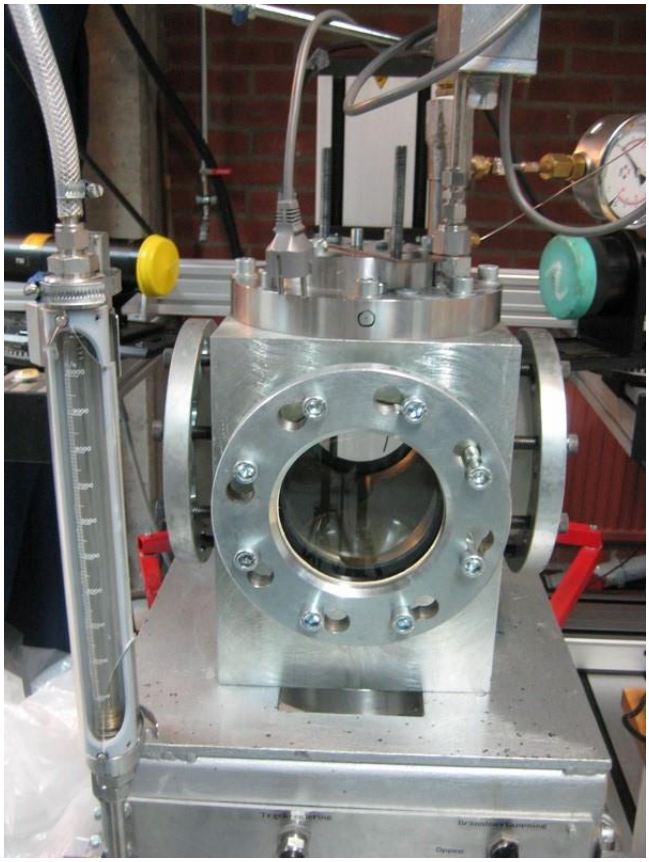

Figure 3: Low pressure spray chamber

2.3 Injector & Injector driver

For all the measurements a prototype multihole injector was used. The injector is aimed for gasoline direct injection systems and is a solenoid actuated, multihole injector with six holes in a symmetrical configuration. The maximum injection pressure according to the specifications can reach 20MPa.

In order for the injector to operate, an external injector driver is needed, which modifies the clock generator pulse to an appropriate signal for the injector. It is made by the same company that provided the injector and is powered by a 12V power source. The output signal reaches 40V and maximum of 10A. No more specifications were available for this injector driver.

Figure 4: Injector, hole configuration

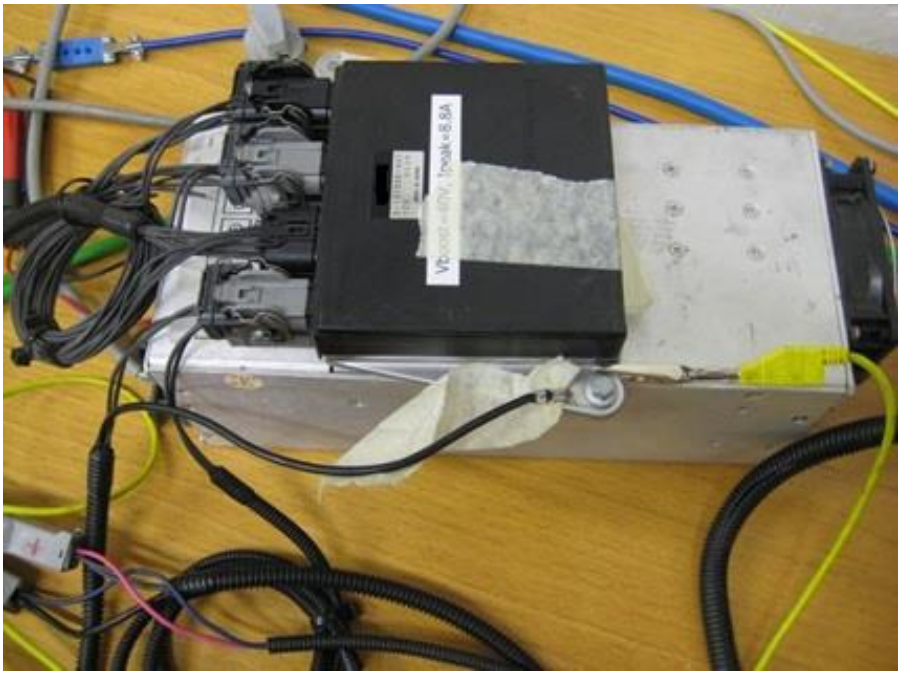

Figure 5: Injector driver and power supply

2.4 High pressure pump

Although the injector during the actual operation in an engine is operated with the use of a mechanical high pressure pump, in a laboratory set up that is not possible. The best solution for the configuration that was used, was to operate the injector with the use of an air driven pump. For all the measurements an air driven Haskel pump was used. By connecting the pump output to a pressure accumulator, fuel pressures of up to 200Bar could be reached. The fuel is fed to the pump from an external fuel tank.

Figure 6: High pressure pump

2.5 Fuel

The fuel that was used in all of the measurements was n-heptane. N-heptane is a widely available testing fuel and as a single component fuel has constant characteristics compared to gasoline 95 octane blends, which as a multi component fuel possess different properties when different samples are used and might affect the final results, mainly the refractive index which is the most important value for accurate results when testing in a spray chamber. The properties of n-heptane are summarized in the following table:

Table 1: n-Heptane physical properties

Molecular formula	C_7H_{16}
Density	679,5 kg/m^3
Vapor Pressure	5,33 kPa
Viscosity	386 µPa*s
Refractive Index	1,387

3 Methodology - System configuration

3.1 Phase Doppler System configuration and calibration

In order to have accurate and reliable measurements the measuring equipment must be configured and calibrated according to the manufacturer specifications. Regarding the Phase Doppler Anemometry system the division of combustion in the department of applied mechanics upgraded the old system with a newer system that had to be configured and calibrated. The laser transmitter part of the system was accompanied by an internal beam expander, an external beam expander and two different focusing lenses, one with 500mm focal length and another with 250mm focal length. Without the use of the focusing lenses the beams would be parallel to each other. The lenses converge the laser beams to create the measuring volume. The focusing length (f) is the distance that the beams converge, measured from the end of the lens. In general the position that the beams converge is called focal point (F).

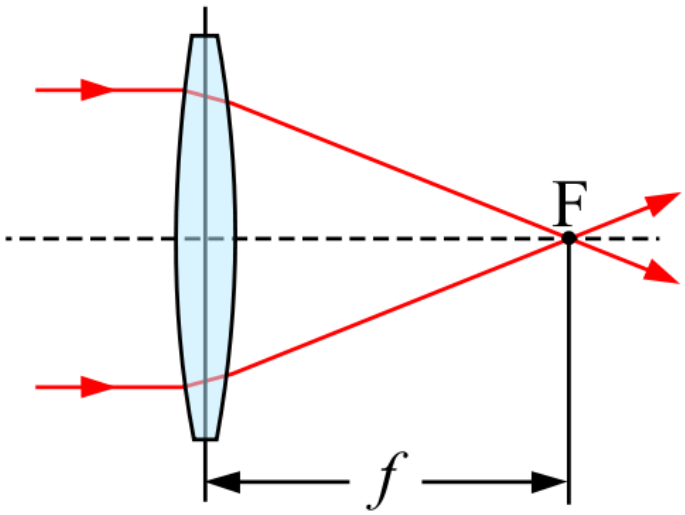

Figure 7: Definition of focal length and focal point

Two different configurations had to be evaluated. The first one would require the use of the external beam expander, the internal beam expander and the 500mm lens. Such configuration would allow the measurements of droplets between 0,5 and 100μm and would allow a better positioning of the whole system around the spray chamber. The off axis angle was selected at 65 degrees, a set up that was used with previous measurements. The evaluation of the setup with the use of a water atomizer outside the spray chamber revealed poor data rate on both measuring channels. Therefore it was necessary to perform calibration of the beams overlap. In order to perform an accurate calibration the transmitter had to be removed from the traverse and placed on a straight sapa aluminum beam. Since the system was dismantled it was suggested to verify the accuracy of the two available beam expanders. As the name implies, the expander increases the distance between two parallel beams. Without any expander the distance between the two beams, named also as beam separation distance, of the same channel should be 20mm at the end of the transmitter and should not deviate up to a distance of 5m. The internal expander gives a 2X expansion ratio so the beam separation distance should be 40mm and the external beam expander has a 2,11X expansion ratio therefore 42mm is the beam separation distance. Testing showed that

while the transmitter without any expanders and with the use of the internal expander performed within specifications, on the other hand the external expander distorted the beams slightly so it was decided to continue only with the internal beam expander. Using only the internal beam expander limits the available focusing lens options only to the 250mm lens.

The beam calibration was performed after the accuracy verification of the expanders. The laser beam was projected on a wall 3 meter away. At the focal point of the transmitter, optical equipment was placed, named microscope object that magnifies the beams so as to be more visible. When tested it was clear that each pair`s overlap and the overall beam overlap was not acceptable. Poor overlap quality affects the number of fringes that are created and there is a major signal loss as a result. According to the manufacturer the minimum acceptable overlap is 80%. In order to adjust the beam overlap the external casing of the transmitter was removed and with the use of a 0.035 ball driver tool the beams were adjusted according to the instructions. The power output during the beam adjustment should not exceed 300mW.

After the beam overlap adjustment it was suggested to check the beam polarization, since polarization affects the maximum fringe contrast of each pair of beams. Still a difference of up to 25 degrees between each plain of polarization is acceptable, because the fringe contrast does not reduce more than 90% of the maximum value. The beam polarization can be verified with the use of the microscope object and a special lens called Polarization Axis Finder. When the Polarization Axis Finder is placed in front of the beam an "X" shape is projected on the wall and indicates the plane of polarization. While the first channel, green, that measures the diameter and the vertical velocity had a stable polarization, the second channel, blue, seemed to have an unstable polarization in one of the two beams, more than 25 degrees that was also affected by the movement of the transmitter on the traverse system. It was later verified by the TSI personnel that came to help configure the system that one of the fibers from the second channel was damaged and had to be replaced.

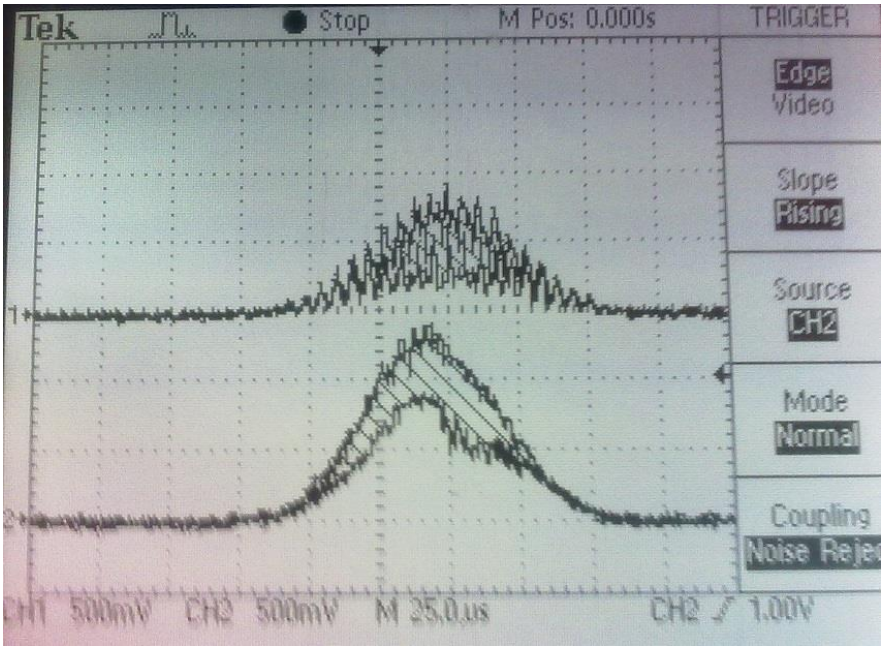

Figure 8: Burst signal through oscilloscope, upper signal is first channel, lower signal is second channel

After the calibration, a new test with the water atomizer revealed that the date rate had increased, meaning that the beam overlap adjustment was successful. Next step was to adjust the system for use in conjunction with the spray chamber. Since the spray chamber has thick glasses in order to withstand high air pressures, the laser beam path is distorted due to light refraction and the off axis angle has to be adjusted. The adjustment proved to be minor and the off axis angle from the original value of 65 degrees was adjusted to 66,5 degrees. A test measurement with the water atomizer revealed that due to the windows the date rate was reduced significantly. Although the first channel data rate was acceptable, the second channel data rate was affected both by the poor polarization and the effect from the windows. Finally the performance of the system would be evaluated when the actual injector was tested.

In order to position the injector correctly into the spray chamber, a brass injector mounting is used. The mounting that was available at the time had different internal dimensions and did not match the injector. A new mounting was machined at the department`s workshop keeping the same external dimensions and had an inside geometry to fit the specific injector.

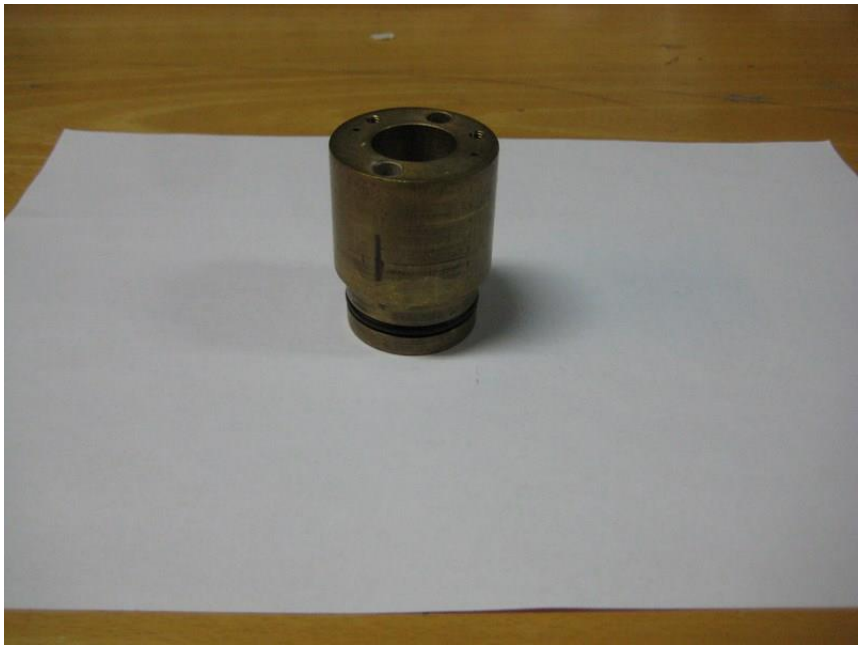

Figure 9: Lower injector mounting

Figure 10: Lower injector mounting, side view

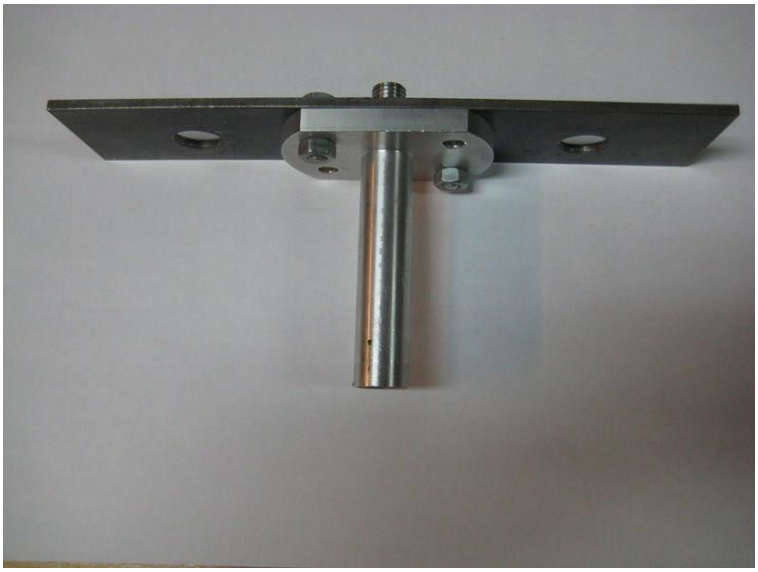

Figure 11: Upper injector mounting

In order to keep the injector secure in the spray chamber and supply it with fuel an upper injector mounting is used. The mounting that was available could not reach the injector because it was short and the injector was positioned low in the spray chamber. A new aluminum upper injector mounting was manufactured with the upper part having a threaded pattern to fit the fuel rail. In order to check that the connection is secure the high pressure pump was connected and the pressure was increased gradually up to 200 bar to check for leaks in the fuel circuit. Afterwards the injector is connected to the injector driver and the injector driver is connected to a Stanford clock generator.

Before starting the actual measurements the injector spray had to be aligned regarding its relative position to the spray chamber. It was placed in a position that would make three of the six fuel plumes visible through the side windows. Since the injector has a symmetrical spray shape, this configuration would make it easier to take high speed images of the spray having three of the plumes overlap the other three.

In order to be able to acquire high speed images as well as phase Doppler data, the injection must be synchronized with the measuring equipment. A Stanford clock generator was used for this purpose. It provides four signal outputs, as well as combined outputs. For the high speed imaging both the injector and the camera were synchronized with the use of an external clock. For the Phase Doppler measurements the FSA4000 processor has its own internal clock and support through the flowsizer software so it only requires the external trigger signal. The start and stop of the sample acquisition is managed by the internal RMR (Rotating Machinery Resolver) function. A rotating encoder translates the signal period into a 360^o duration and the start and stop signals are adjusts as degrees of the 360^o duration. After a couple of measurements it was observed that the RMR function did not operate properly and was capturing droplets outside the measuring time range. After suggestions from TSI, a different synchronization method was used where all the signals come from the clock generator. The trigger signal T_0 is fed to the FSA4000 through the Sync Pulse input while the measuring duration is fed to the Burst Inhibit input using a combined signal of negative flank (in this case $C \cup D$) .

3.2 Measurements - Experimental procedure

3.2.1 High speed imaging

For the high speed imaging the injection pressure was the only varied parameter. Four different pressures were tested, 50bar, 100bar, 150bar and 200bar. The backpressure was kept constant at 1,1 bar and the injection duration was 1,5ms.

Images were taken at 14.000 frames per second for 3ms duration with a resolution of 320x344 pixels. Thirty images were saved as a multi-tiff file where it could be observed the injection delay, the main injection and the droplets that appear after the injector closes.

The equipment used was a Phantom high speed camera positioned in front of the injector while the illumination was provided from the rear with the use of two spot lights through a diffuser plate.

3.2.2 Phase Doppler Interferometry – Droplet sizing

3.2.2.1 Influence of fuel pressure

The measurements for the influence of the fuel pressure had one variable, the fuel injection pressure. The tested pressures started from 25bar to 50bar, 100bar, 150 bar and reached 200bar. The injection duration was constant at 1,5ms, each injection had a four second period (0,25Hz frequency) and backpressure was kept at 1,1bar. Temperature was between 21^{o}C to 23^{o}C. The laser power that was used was 750mW and the measuring time was defined as 3ms after the trigger signal to the injector. Air flow through the spray chamber was at 1500lt/h in order to have quiescent air conditions.

Before starting the actual measurements a PMT voltage calibration was performed as it is described in the TSI manual. With constant injection pressure, the PMT voltage is varied between 400V to 650V and the D10 diameter is calculated. At low voltages small droplets do not get enough amplification from the system and are not counted as valid droplets and as a result D10 value is high. At high PMT voltages noise is amplified and is counted as valid droplet and the D10 value increases again. As the PMT voltage increases the D10 value reaches a minimum value. That PMT voltage is used for the actual measurements and in this case this was 575V.

3.2.2.2 Influence of injection duration

In this case the influence of injection duration on droplet diameter and velocity was examined. Three different durations were evaluated, 1,5ms, 3ms and 5ms duration while the pressure was constant at 100bar. The configuration that was used in the previous measurements was used, 750mW laser power, 1500lt/h air flow, backpressure of 1,1bar, 0,25Hz injection frequency. The measuring time was adjusted according for each injection duration and it was 3,5ms for the 1,5ms duration, 5ms for the 3ms injection and 7ms for the 5ms injection. The spray core position as well as the adjacent positions were the same that were used for the 100bar pressure during the pressure influence measurements.

3.2.2.3 Influence of double injection

The first aim of this measurement was to see if the specific injector was able to perform a double injection event. If that was feasible then it had to be evaluated the minimum duration between each injection event.

For the double injection the available clock generator was not enough so a second more advanced clock generator was used. The first clock generator was used to provide the trigger for the TSI FSA4000 measuring equipment and feed the same trigger pulse to the second clock generator that was controlling the double injection.

The measuring pressure was again 100bar and all the other conditions were the same with the previous measurements. The duration of each injection was 2ms while the duration between each injection was 1ms. The total measuring time was 7ms.

3.2.2.4 Evaluating the injector spray – measurement positions

For each pressure level, injection duration and for the double injection, data from five different positions were acquired. The middle position, or the spray core and another four positions, two before and two after the spray core. For all the measurements the vertical distance from the injector nozzle was at Z=30mm downstream. For the spray core 15.000 droplets were validated and for the other four positions, 5.000 droplets were validated for each position.

3.2.2.5 Identifying the spray core position

Since the available injector could produce six independent fuel plumes, it was decided to evaluate plume number 2' because it was the easiest accessible for the Phase Doppler system, inside the spray chamber. Using the Sprayvis software a matrix of forty different positions was created and tested. For each position 500 droplets were acquired and after processing the results the spray core was identified for each injection pressure.

Figure 12: Six hole multihole injector, nozzle tip

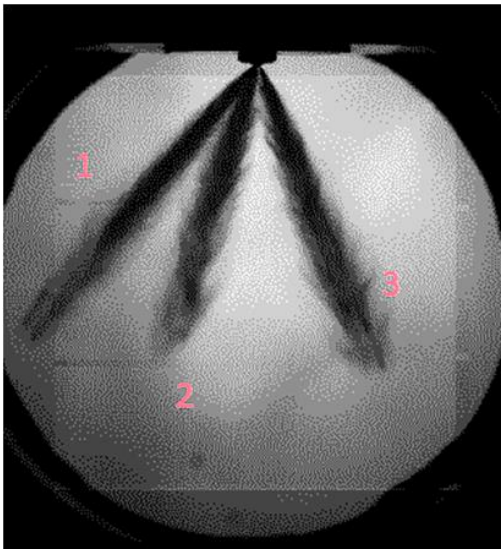

Figure 13: Identification of plumes relative to the injector

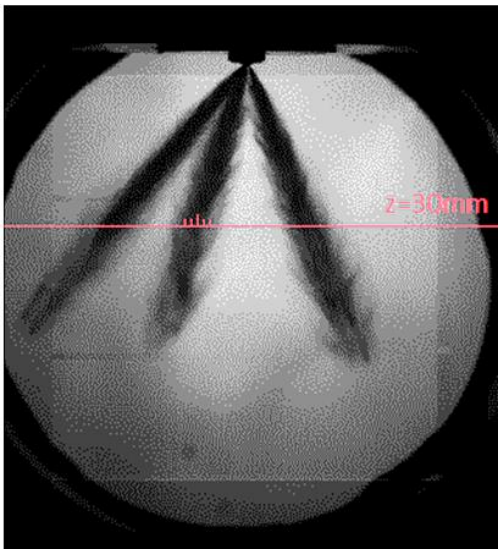

Figure 14: Five measuring positions at 30mm

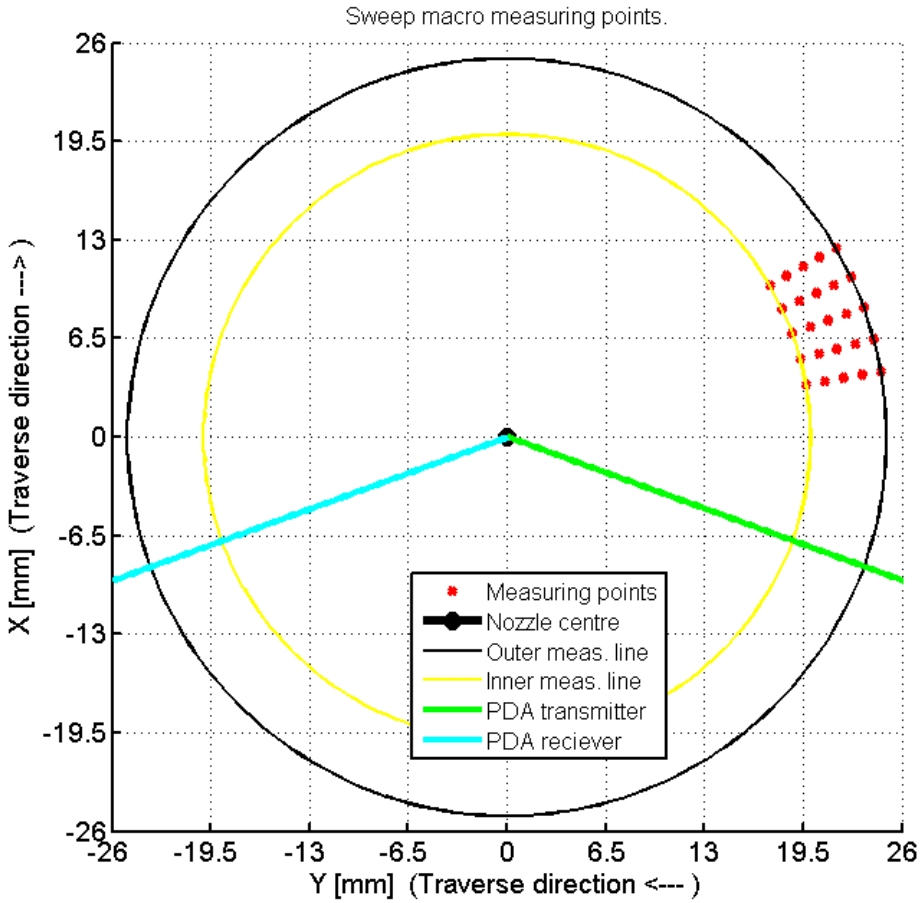

Figure 15: Example of a test matrix from Sprayvis

3.2.2.6 Processing the data

When capturing PDA data from a direct injector, the droplet velocity VS time graph, after many consecutive injections, would look like the following.

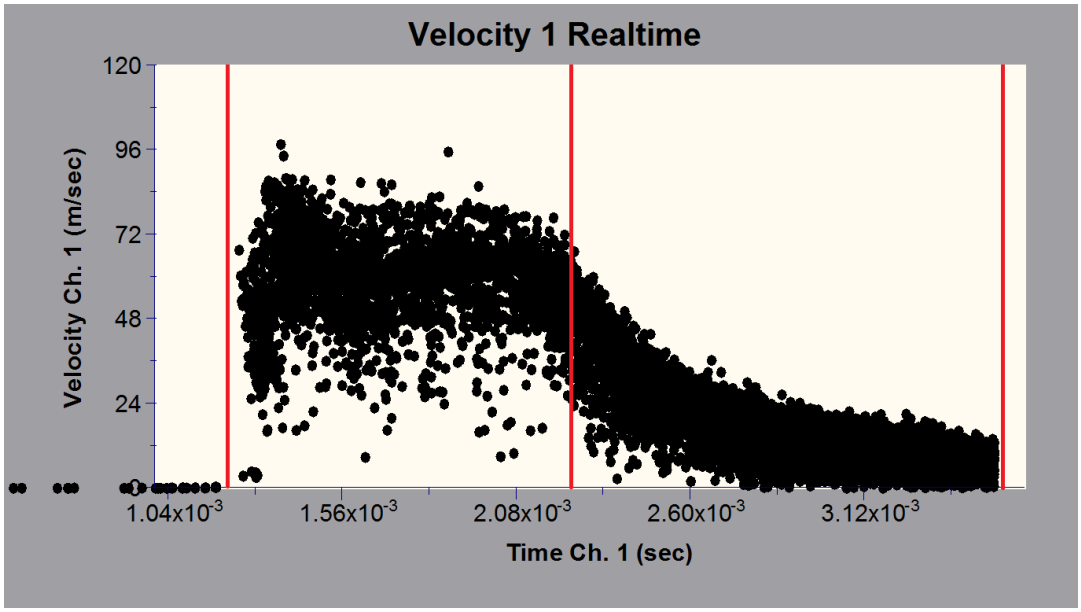

Figure 16: Velocity VS time graph, highlighting the two different injection parts

The injection event can be divided into two parts. The main part of the injection which contains the fuel droplets that are created while the injector nozzle is open and the second part which contains slow moving droplets that are created just before the injector closing as well as recirculated droplets inside the chamber from the previous injection. In order to evaluate the injector properties and performance, only the main part must be taken into account. Therefore a reduced droplet sample of 1ms duration was used for data processing. As the injector pressure increases the droplets have different velocities and require different time to reach the measurement volume. Because of that the processing time start and stop is different for each pressure level and can be summarized as follows:

Table 2: Starting and ending timings for data processing at different injection pressures

Pressure (bar)	Start (ms)	Stop (ms)
25	1,6	2,6
50	1,3	2,3
100	1,2	2,2
150	1,2	2,2
200	1,2	2,2
100 – 3 ms duration	1,2	4
100 – 5 ms duration	1,2	5,8
Double – 1st injection	1,2	2,8
Double – 2nd injection	4	5,6

The corresponding results for the D10, D32 and $V_{average}$ were calculated with the use of SprayVis software for each reduced droplet sample.

4 Theory - Literature review

4.1 Phase Doppler Anemometry Theory

When conducting experiments, involving liquid flows, it is necessary to be able to measure the velocity of the flow with high accuracy and if the flow contains solid particles or is atomized such as a spray, it is important to know also the droplet diameters that are part of the spray. One of the best methods available for such measurements is a laser optical method known as Laser Doppler Anemometry and the extension of that method, the Phase Doppler Anemometry. The advantage of Phase Doppler Anemometry compared to the Laser Doppler Anemometry is that both the velocity and size of spherical particles can be measured at the same time. As a result the Phase Doppler Anemometry can be used to investigate the velocity and droplet distribution of water or fuel sprays as well as solid spherical particles in liquid flows.

4.1.1 Principles of Phase Doppler Anemometry

The first publication regarding the principles of a PDA system were presented by Durst and Zaré (1975) and then followed by publications focused on technical descriptions of the system as well as applications on two phase flows. The most notable are by Bachalo and Houser (1984) and Bauckhage and Flögel (1984).

The main principle that the Phase Doppler Anemometry is based on, is the scattering of light from moving particles. Although the light scattering mechanisms consist of reflection, refraction and diffraction, for PDA measurements reflection and first order refraction are considered as the most important. In the case of refraction, the refractive index **m** which is defined as the refractive index of the particle divided by the refractive index of the surrounding medium ($m= n_p/n_m$) is important as well and in the case of liquid droplets in air or gaseous substance is higher than 1 ($m>1$).

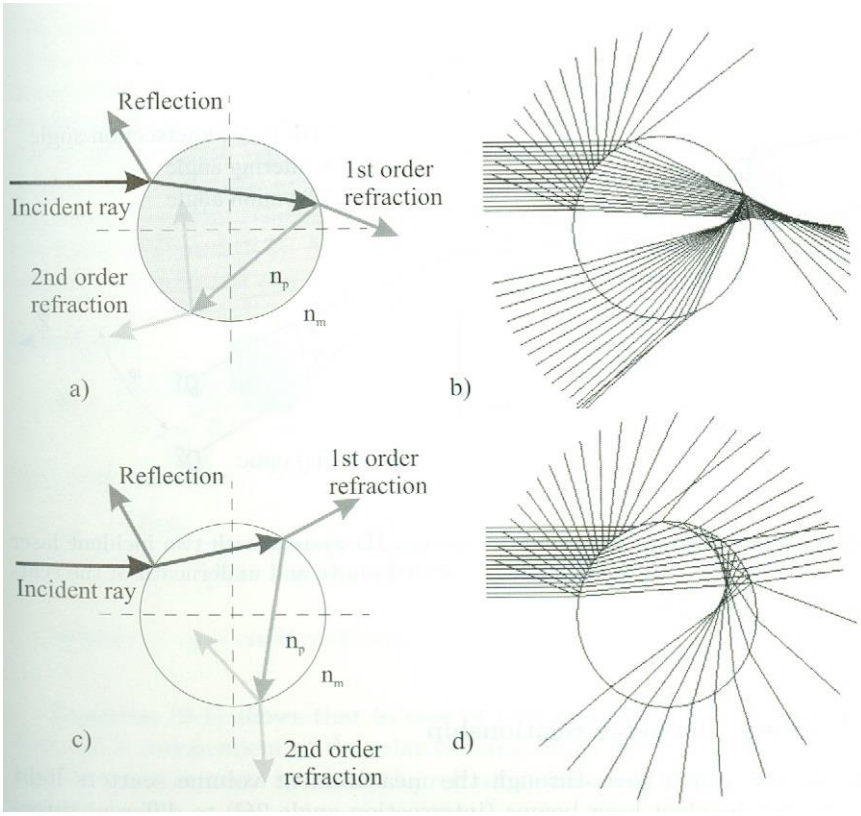

Figure 17: Reflection and refraction

4.1.2 Velocity measurement - Laser Doppler Anemometry

Both measuring techniques work with the same principle for measuring velocity in three directions. Because of that, the principles of Laser Doppler Anemometry will be described and can be directly applied to Phase Doppler Anemometry.

Laser Doppler Anemometry can be considered a non-invasive, single point measuring method. It is considered an absolute measuring method and as a result no calibration is required beforehand. As a result it can be used for flow measurements in applications that methods such as hot wire anemometry or Prandtl probes are unsuitable.

The Laser Doppler Anemometry is based on the principle that when a particle passes from a light source will scatter light that will have a frequency shift compared to the original light source. This effect is known as the Doppler Effect. The most common method/system is the dual beam, where a laser beam is split into two parts. Afterwards the two beams of wavelength λ are focused to the same point, creating the measuring volume. Since both beams intersect to create the measurement volume an angle θ appears between them which is crucial in calculating the velocity of the particle or the droplet. When a droplet passes through the measuring volume, it scatters light that has a frequency shift compared to the original light, due to the Doppler effect and is referred as beat frequency (f). The scattered light is then detected by a photodetector and from the beat frequency the velocity of the particle can be calculated directly.

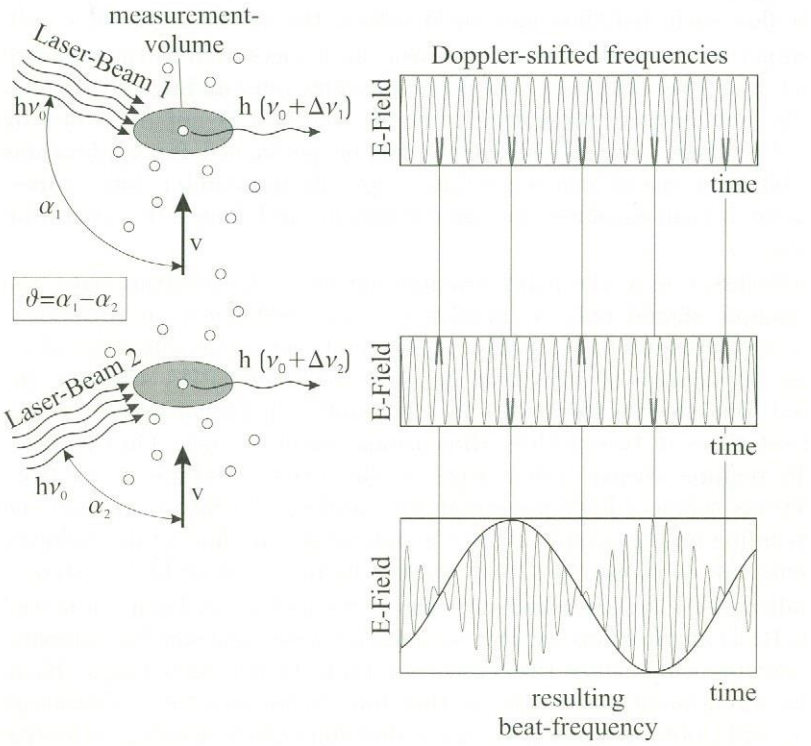

Figure 18: Doppler shifted frequencies

$$v = \frac{f\lambda}{2\sin\frac{\theta}{2}} \quad (1)$$

4.1.3 Bragg cell - fringes - optics - measuring volume characteristics

A major problem with this technique is that it cannot distinguish between a positive and a negative velocity since both of them create the same Doppler frequency shift. In order to overcome this drawback one of the two laser beams is shifted in frequency by adding a shift frequency fs. As a result the superposition of the two beams creates a resultant wave that has bright and dark peaks called fringes and is moving from the shifted beam to the unshifted beam with a velocity of V=λ*fs. As a result a passing droplet with positive velocity, through the measuring volume now will have a Doppler frequency higher than the shift frequency whereas an droplet of negative velocity will have a Doppler frequency that is lower than the shift frequency. Therefore the velocity can be calculated by the following equation:

$$v = \frac{(f - f_0)\lambda}{2\sin\frac{\theta}{2}} \quad (2)$$

In an actual laser doppler system the frequency shift is achieved with the use of an acousto-optical modulator, which is known as the Bragg Cell and the most common shifted frequency is 40MHz. The laser system that is most commonly used consists of an Ar-ion laser system that has a maximum power output of up to 10W that can produce laser light at three precise wavelengths, 488nm, blue, 514,5nm, green, 476,5nm, purple and each of them is used for the measurement of each velocity component in a 3D flow. The measurement volume that is created by the laser beams can be considered an ellipsoid with an Gaussian intensity distribution. Therefore the dimensions of the measuring volume can be calculated if the laser beam diameter dl and the beam intersect angle θ are known.

$$d_x = \frac{d_l}{\cos\frac{\theta}{2}} \quad (3)$$

$$d_v = dl \quad (4)$$

$$d_z = \frac{d_l}{\sin\frac{\theta}{2}} \quad (5)$$

also another important length, the fringe distance d_f can be calculated as:

$$d_f = \frac{\lambda}{2\sin\frac{\theta}{2}} \quad (6)$$

and finally the number of fringes (N_f) inside the measuring volume can be derived by

$$N_f = \frac{d_x}{d_f} = \frac{2d_l\tan\frac{\theta}{2}}{\lambda} \quad (7)$$

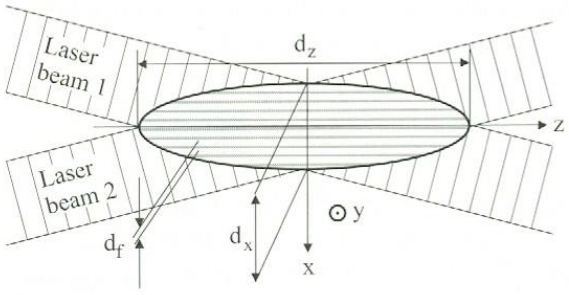

Figure 19: Measuring volume

4.1.4 Diameter measurement - Phase Doppler Anemometry

As an extension to the previous technique, Phase Doppler Anemometry determines the size of spherical particles or droplets by analyzing the frequency shift of the scattered light that is created when a droplet passes through the measuring volume that is created by at least two laser beams. The size measurement is based on the fact that the scattered light that is received by at least two detectors has a phase difference which is proportional to the diameter of the droplet.

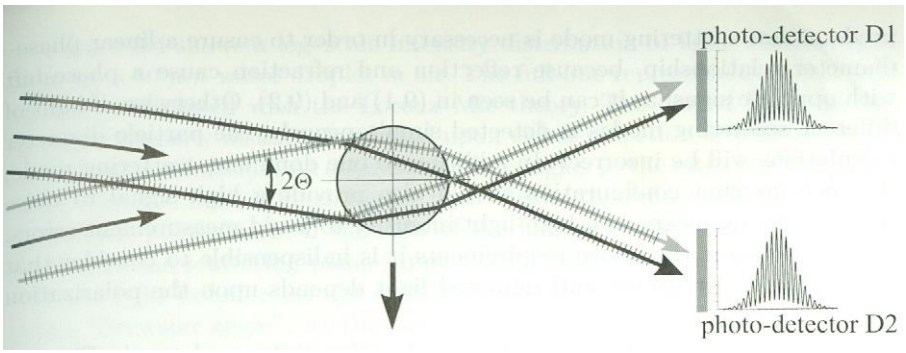

Figure 20: Photodetector signals

As with the laser Doppler anemometry system, the important parameters that have the greatest influence in the diameter measurements are the beam intersection angle, θ, the scattering angle φ, (known also as off-axis angle), the elevation angle Ψ, the polarization of the laser beams and the detector aperture size.

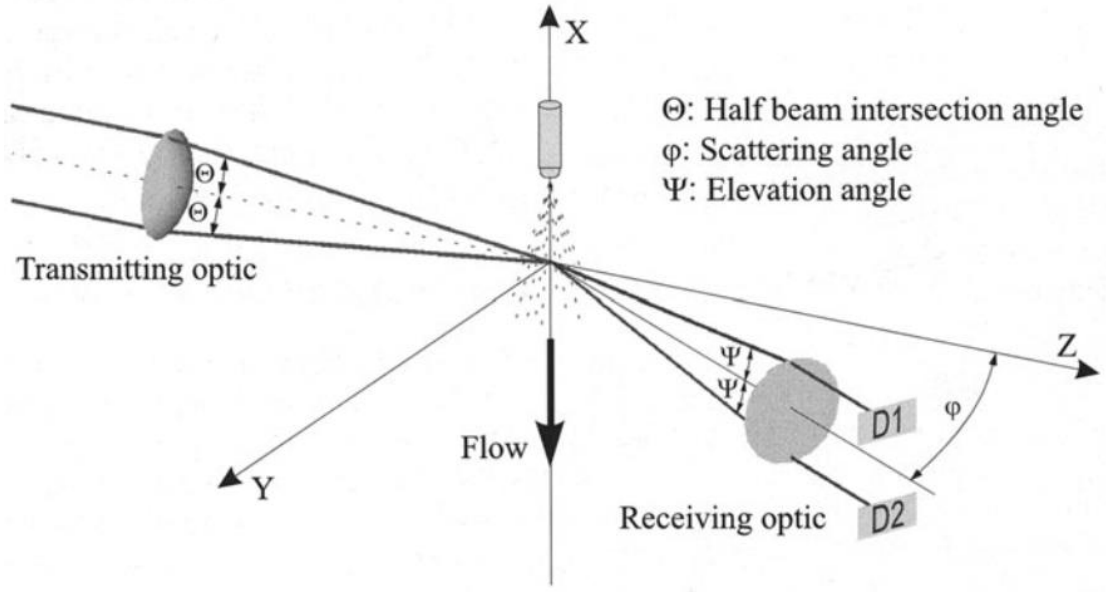

Figure 21: Simple schematic of a Phase Doppler Interferometry system

In Phase Doppler Interferometry instead of having only one photo-detector it is necessary to have at least two. The distance that refracted light has to travel depends on the relative position of each photo-detector to the droplet. Because the photo-detectors are located in different positions they receive the Doppler burst, the same that is used for velocity calculations, at different time, or with a phase difference. It has been proven by the early research topics on phase Doppler interferometry that this phase difference has a linear correlation with the droplet diameter. Therefore a large droplet causes a large phase difference and vice versa for small droplets. Moreover this linear relationship is valid both for reflected and refracted light and exact mathematical equations can describe this phase-diameter relationship.

Reflection:

$$\Phi = \frac{2\pi d_p}{\lambda} * \frac{\sin\Theta \sin\Psi}{\sqrt{2(1-q)}}, \qquad \sin\Theta \sin\Psi \ll q \quad (8)$$

Refraction, 1st order:

$$\Phi = \frac{2\pi d_p}{\lambda} * \frac{m \sin\Theta \sin\Psi}{\sqrt{2(1+q)(1+m^2 - m\sqrt{2(1+q)}}}, \qquad m > 1 \quad (9)$$

$$\text{and } q = \cos\Theta \cos\Psi \cos\varphi \quad (10)$$

To ensure more accurate results it is necessary to have only one dominant scattering mode and high quality signals in terms of signal to noise ratio. That can be achieved by selecting carefully the laser beam polarization plane and the scattering angle φ, since they have a major effect on the intensity of the reflected or the refracted light. As it was mentioned before, when only one scattering mode is the dominant the phase-diameter relationship is linear.

The phaseshift can have values between 0^o and 360^o and as a result there is a specific maximum diameter that can be measured and is dependent on the gradient of the phaseshift vs diameter diagram. Larger droplets that have phaseshift greater than 360^o will be recognized as (phaseshift - 360^o) which will cause measurement errors. For example a droplet with 500^o phaseshift, will be recognized as 500^o - 360^o = 140^o. To overcome this problem a third detector is used and is usually placed close to the first detector. This results in a smaller phaseshift between detector one and detector three which gives a lower gradient in the phaseshift vs diameter diagram. Consequently with this addition measurements over 360^o are validated by the third detector. As a result a three detector system can provide high resolution and accuracy for small particles as well as large diameter range. (Mayinger & Feldmann, 2001)

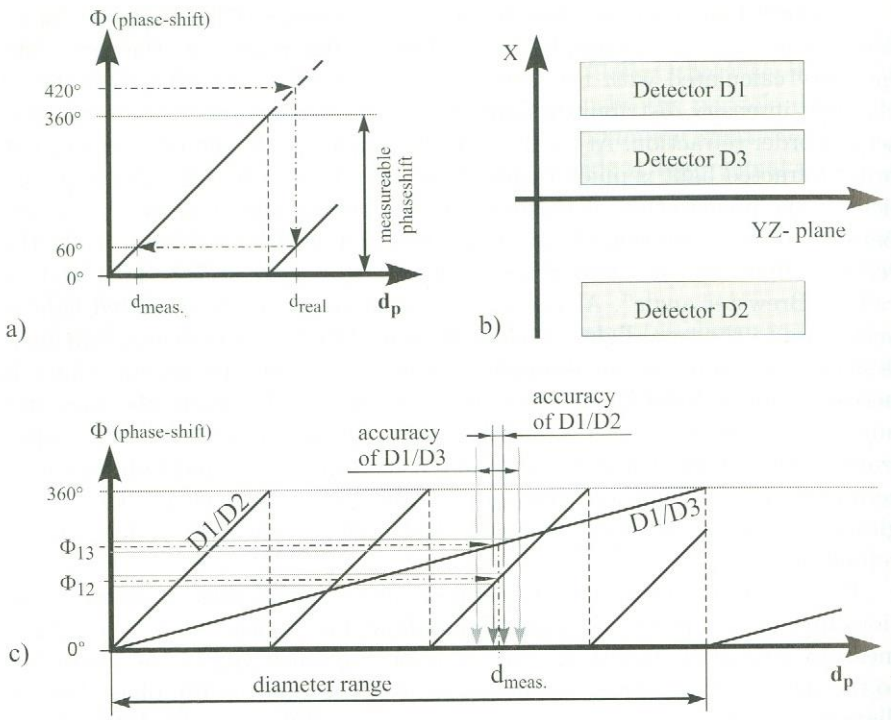

Figure 22: Three detectors accuracy improvement

Although a Phase Doppler Interferometry system can calculate the diameter of each droplet, in an actual measurement more than 10.000 droplets might be needed in order to have accurate results. Because of that there are two different diameter metrics that are used to give an average droplet diameter for the sample. These are the D10 or $D_{1,0}$ or arithmetic mean and D32 or $D_{3,2}$ or SMD (Sauter Mean Diameter). They are defined as follows:

$$D_{10} = \frac{1}{n}\sum_{i=1}^{n} di \quad (11)$$

$$D_{32} = \frac{\sum_{i=1}^{n} di^3}{\sum_{i=1}^{n} di^2} \quad (12)$$

Sauter Mean Diameter is defined as diameter of a sphere that has the same volume / surface area ratio as a particle of interest and it is especially important in calculations where the active surface area is important.

4.2 Gasoline Direct Injection – Systems and Injector Types

In the last fifty years the internal combustion engine has become the main means of vehicle propulsion, where the spark ignition engine dominates the passenger car industry and the compression ignition engine is the norm for heavy duty engines, ranging from small truck engines to large ship engines. With the increase in the number of vehicles the last twenty years, new problems have appeared in terms of depletion of fossil fuel resources and the increase of the harmful engine emissions as well as the emissions which are a major contributor to the global climate changes. As a result the European Union has taken measures to reduce fuel consumption and carbon dioxide emissions down to 130g/km for year 2015 and below 95g/km by 2020.

One of the major boost in the reduction of fuel consumption from a spark ignition engine was the introduction of port fuel injection (PFI). In this system the fuel is injected at a relatively low pressure of up to 4bar in the intake ports before the valves open for the intake stroke. The atomized fuel then evaporates and mixes with the intake air, creating a homogeneous mixture before entering the cylinder. While port injection is a cost effective system with adequate performance, it lacks certain characteristics that can help reduce the carbon dioxide emissions even further as well as it does not provide optimum transient response under rapid increase in the engine load, as in an acceleration event. From a thermodynamic aspect port fuel injection provided limited cooling effect during the evaporation of the fuel and as a result the engine operation at high loads in knock limited. A further implication of that fact is that the engine compression ratio, which has a positive effect on the efficiency, can only accept a limited increase in its value.

A major improvement from the port fuel injection concept is the direct fuel injection, meaning that the fuel is injected directly into the cylinder. Although the first concepts of a gasoline direct injection engine appeared back in 1954, the lack of advanced electronics and engine control systems meant that the first commercially available direct injection engines appeared during the late 1990, at first by Mitsubishi with the GDI branding and later by many other major manufacturers.

The adoption of direction injection enabled the manufacturers to adopt advanced injection strategies with the most common being the direct injection stratified charge (DISC). This ultra-lean operation mode can be used at low loads and speeds and creates a combustible mixture in a limited area in the cylinder, filling the rest of the cylinder either with air or cooled exhaust gases (EGR). During this mode of operation the efficiency increases due to the reduction of pumping losses because the engine operates unthrottled and the reduction of the cooling losses because the exhaust gases or the excess air acts as an insulator therefore decreasing the heat losses to the surroundings. The use of high pressure direct injection provides more benefits as well. The combustion timing can be better controlled since there is not the time delay associated with the PFI between fuel injection and intake of the fuel/air mixture in the cylinder. That can help the engine operate with less cycle to cycle variations and improve the transient response. Finally, injecting the fuel directly in the cylinder can help decrease the intake air temperature since the fuel absorbs heat from the air in order to vaporize. Because of this cooling effect the compression ratio can be increased compared to a PFI, which increases the thermodynamic efficiency even further.

All these benefits of the direct injection engine can provide a theoretical reduction in fuel consumption of up to 25% compared to a conventional engine. In reality during the New European Driving Cycle (NEDC) tests the fuel consumption reduction can reach up to 20%, establishing the potential of the direct injection engine.

While direct fuel injection has the advantages mentioned before, there are also drawbacks. Since the engine can operate in many different modes such as stratified or stoichiometric, the injectors must be able to perform optimally under all conditions. A problem that can arise is that the fuel might over penetrate and hit the cylinder wall or the piston causing high carbon monoxide and unburned hydrocarbon emissions. Moreover, due to the limited amount of time that is available for the injection high fuel pressures must be used, which increases the parasitic losses and requires expensive high pressure fuel pumps and sophisticated engine control systems.

In order for the direct injection systems to be able to perform under stratified operation three different systems have developed over the years and differ in the way of mixture preparation and its transport towards the spark plug for combustion. These different systems are categorized as:

- Wall-guided systems
- Air-guided systems
- Spray-guided systems

4.2.1 Wall-guided systems

These systems are characterized by a wide spacing between the injector and spark plug. The fuel is injected during the compression stroke and is guided to the spark plug mainly by the piston crown and secondary by the air and spray motion inside the cylinder. The spray shape is not so important in this system since the spray movement promotes good mixture homogenization.

Main drawbacks of this system is that there is long time interval between injection and combustion, which can cause overmixing at low engine speed. At high loads and speeds parts of the fuel might reach the cylinder walls. Moreover because the fuel comes in contact with the piston crown a liquid film of fuel might develop on the piston which can lead to partial combustion, thus creating carbon monoxide, soot and unburned hydrocarbons and high fuel consumption.

In order to be efficient such a system, the spray, the piston geometry and the in cylinder air motion have to be optimized for different loads and speeds. One of the first engines that used this kind of system was the Mitsubishi GDI engine, which used a swirl type injector for the fuel delivery.

4.2.2 Air-guided systems

The next evolution of direct injection systems is the air guided systems. With these systems a well-controlled air motion transports the fuel for the injector to the sparkplug. Since air motion is the predominant mechanism of fuel transportation the way it is created and controlled is very crucial.

In order to be able to control the air motion, in an air guided system, a variable tumble system is present in the intake pipe, that controls the tumble motion of the air and guides the fuel/air mixture near the sparkplug. Major constrains for such system is the cyclic variations of the mixture motion which hinder the use of stratified operation at a wide engine operating range, as well as fine tuning the design of the intake pipe and the combustion chamber. Still the air guided systems provide fuel economy benefits of up to 15% compared to a PFI engine and up to 10% compared to a wall guided system.

4.2.3 Spray-guided systems

The most recent advancement in direct injection systems is the spray guided systems which seem promising in delivering the fuel economy benefits from direct injection. Compared with the previous systems, in a spray guided system only the spray shape that is created from the injector is responsible for the proper air and fuel mixing and transportation of the mixture in the vicinity of the sparkplug for combustion, while the geometry of the piston crown and the air motion have negligible contribution.

Still for the spray guided systems, two different approaches have been developed. First is the close spacing concept, where the injector is placed close to the spark plug, usually in a vertical position. This approach gives good control over the injection timing and ignition, minimizing the cyclic variations due to small influence of the air motion to the mixture formation, making possible the stratified operation range to be extended and minimize UBHC emissions.

The second approach is the wide spacing concept, where the fuel injector is placed at the side of the cylinder and spark plug is centrally located. Such a system has better resistance in injector deposit formation due to lower injector tip temperature and can provide better mixture stability near the spark plug.

The spray shape and atomization of the fuel are crucial in a spray guided system since the air/fuel mixture has to be between acceptable limits and no liquid fuel must reach the spark plug, which can cause misfires or fouling. Also due to limited time between injection and ignition the spray must be able to mix quickly with the air without creating over mixing or under mixing areas. Finally the spray distribution within the cylinder must be constant regardless of the in cylinder air motion and conditions.

Nevertheless, in real life applications the manufacturers use a combination of the three different systems.

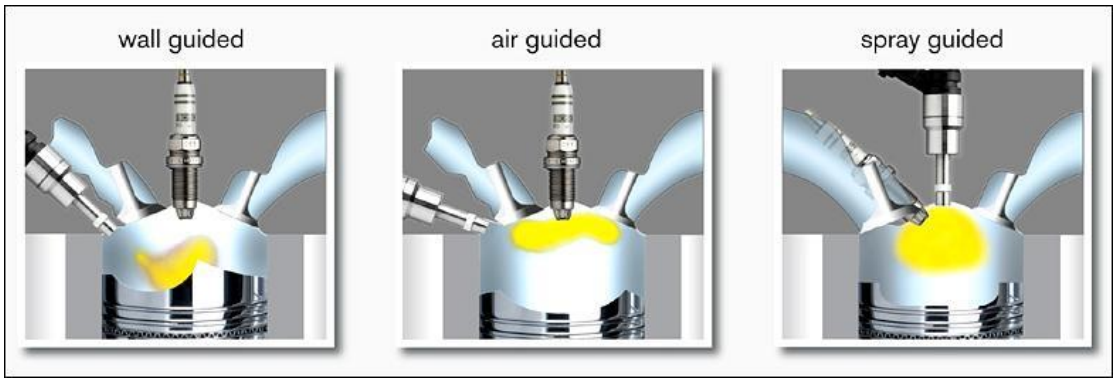

Figure 23: Comparison of three different injection systems (Xander, 2006)

4.2.4 Fuel injector types

It has become obvious that one of the most important components in a direct injection engine is the fuel injector. A fuel injector that is designed for direct injection systems must be able to perform optimally during stoichiometric operation and in some systems during stratified operation as well. The atomization properties of the injector and the spray pattern must be consistent and reproducible throughout the operating range, in order to provide low emission levels, low fuel consumption and reduce the knocking possibility during full load to a minimum.

Since the requirements for the fuel injector are very high, a single design performing optimally is difficult to be found. As a result the last ten years, during which the gasoline direct injection engines have become commercial, many different injector designs have been proposed. Their differences can be found in the spray patterns, the way the fuel is atomized and the opening direction of the control element. Furthermore the injectors can be distinguished by the spray shape that is created with the most common types being the inwards opening swirl type injector, inwards opening multi-hole injector and outwards opening piezo injector (A nozzle). In order to meet the requirements for direct injection applications, all of these injectors operate at high injection pressures, between 50 to 200 bar, while the trend shows a further increase of the injection pressure up to 300 bar.

4.2.4.1 Inwards opening swirl type injector

Swirl type injector is considered one of the first type of injectors created for gasoline engine applications. The injector control element moves inwards and the shape of the nozzle creates a rotational flow leading to a thin film of fuel at the exit of the nozzle. This type of injector creates a jet of fast moving high diameter droplets followed by a characteristic hollow cone umbrella shape. This type of injector creates good atomized particles at low fuel pressures due to the thin fuel film that is created, but the shape of the spray is greatly influenced by the in-cylinder air motion, pressure and temperature. Moreover deposit build up in the nozzle affects the spray shape which reduces the combustion quality.

4.2.4.2 Multi-hole injector

A most recent injector design is the inwards opening multi-hole injector. The main advantage of this injector is that it allows a large variation in the spray shape which is created from the position and orientation of the holes in the injector nozzle. The most common configuration is the symmetrical multi-hole pattern with six or more holes but other configurations are available such as the six hole crescent like shape or symmetrical multi-hole with a center hole.

This type of injector can create multiple thin high speed fuel sprays, while the droplet diameter and atomization quality is governed by the number of holes and their diameter as well as the internal flow. Furthermore the multi-hole injectors have significant advantages. The spray shape can be adapted to the specific engine application. The spray shape geometry is not easily affected by the in-cylinder conditions. Multiple injections are possible and the delay between the signal and the injector opening is around 0,7ms. They are not affected much by deposit built up. However the atomization quality is not so good at low to moderation injection pressures, 25 to 100 bar.

Multi-hole injectors are mainly used with spray-guided engines due to the ability to tune the spray shape to fit the corresponding engine design.

4.2.4.3 Outwards opening piezo injector

The most recent type of fuel injector is the outwards opening piezo injector. The main difference is in the way which the injector needle is actuated. In this type of injector a piezo stack acts directly on the needle, providing a very small delay between the signal and the actuation of the injector, which is around 0,3ms. More advantages of the piezo actuation include the ability to perform multiple injection events and use small injection durations. Furthermore, recent improvements on this type of injector include the ability to adjust the needle lift as well, providing another parameter to control the fuel mass flow as well as droplet sizes.

Because of the outwards opening of the injector needle, the spray has the shape of a hollow cone umbrella. The spray that is created gives very low liquid penetration and has very good stability due to the appearance of toroid vortexes at the spray edge which enhance the fuel transportation near the spark plug area. Still while piezo actuated injectors have many advantages in terms of spray shape and stability, are not widely adopted by auto manufacturers due to difficulty to manufacture and high production costs. (Skogsberg, 2007)

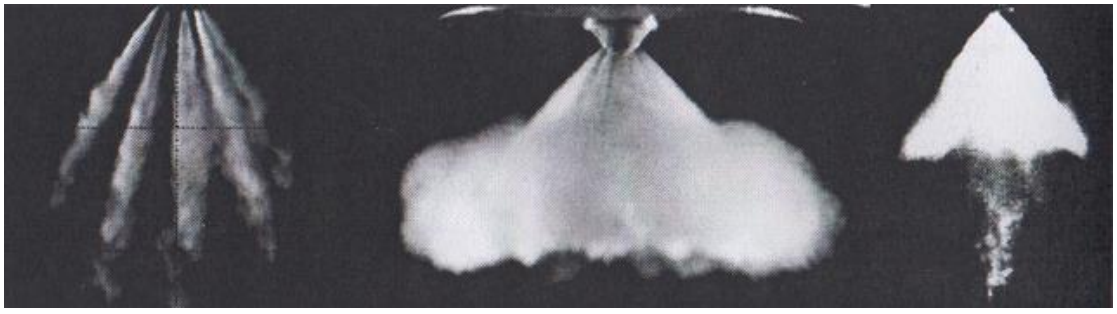

Figure 24: Spray formation from three different types of injector, multihole, outwards opening, swirl type (Skogsberg, 2007)

The properties of each type of injector can be summarized in the following table:

Table 3: Characteristics of three different types of direct injector

	Swirl type	Outwards opening	Multihole
Spray stability	+	++	+
Flexibility of spray pattern	+	O	++
Resistance against backpressure influence	-	++	++
Multi-injection capability	O	+	O
Cost	O	-	+
Robustness against plugging	+	+	+

4.3 Literature Review

Gasoline direct injection is a very promising concept in reducing fuel consumption and exhaust emissions and as it was mentioned before, the injector has a very important role in it. Because of that a lot of publications are focused on the performance of different types of injectors under varying conditions, tested not only inside spray chambers but also under real operating conditions inside an engine.

Since the main focus of this thesis was the performance of the injector under non vaporizing conditions the following papers helped to understand what has been done so far on the specific subject and act as guidelines while designing the measurements and help evaluate the final results.

4.3.1 Paper 1

"An analysis of spray development with iso-octane, n-pentane, gasoline, ethanol and n-butanol from a multi-hole injector under hot fuel conditions" by P.G. Aleiferis and Z.R. van Romunde (Aleiferis & Romunde, 2013)

In this paper a six hole multihole injector, with asymmetric arrangement, was tested amongst other tests, in terms of droplet diameters and velocities at 20^{o}C and 1bar backpressure with the use of iso-octane, gasoline and n-pentane using Phase Doppler Anemometry. The downstream distance from the injector nozzle was 25mm while the injection pressure was set at 150bar. It is observed that due to the non-atomizing conditions the detection rate is not constant. High droplet count is validated when the initial spray reaches the measuring volume but it is reduced significantly afterwards due to the high density of the fuel. The detection rate increases again during the last part of the injection when the injector tip closes and the fuel has reduced velocity and volume. It is noted that the highest diameter of the droplets is detected in the first part of the spray with a decrease in the mean diameter in the following part of the injection. It is noted that the three tested fuels give almost similar SMD (Sauter Mean Diameter), (D32). Gasoline has a D32 of about 17μm, iso-octane gives a D32 of 16μm and n-pentane has the lowest D32 of about 14,5μm.

For the droplet velocities only iso-octane was measured. At 1bar and 20^{o}C the leading part of the spray has droplets with velocities around 40 to 60m/s while the highest velocity of the droplets reaches 90m/s around 0,7ms after the start of injection and the average velocity is around 50m/s.

4.3.2 Paper 2

"Momentum Flux Spatial Distribution and PDA Analysis of a GDI Spray" by L. Postrioti, M. Bosi, A. Mariani and C. Ungaro (Postrioti, Bosi, Mariani, & Ungaro, 2012)

For this paper the researchers used a three hole symmetrical research injector, similar to the commercial available injectors. The operating temperature and pressure is defined as "room temperature and pressure" while the liquid that was used is Exxol-D40. The injection pressures that were used were 50bar, 100bar and 150bar.

Five different Z distances downstream of the injector were used, starting from 10mm and reaching 50mm with a 10mm interval, while the other two coordinates, defined as X=0 and Y=0 were at the middle of one of the plumes.

The results show a minor variation in the droplet diameter, for a given injection pressure, with the diameters for the 50bar injection pressure starting from 8μm (D10), 28μm (D32) at 10mm downstream and having almost the same value at 50mm downstream. Similar results can be observed also for the 100bar with 7μm (D10), 24μm (D32) at 10mm and 7μm (D10), 20μm (D32) at 50mm. 150bar have 6μm (D10), 22μm (D32) at 10mm and 6μm (D10), 14μm (D32) at 50mm.

On the other hand the average velocity changes dramatically as the distance increases with the 50bar injection pressure having 30m/s at 20mm and reaching 19m/s at 50mm and the 150bar injection pressure giving 50m/s at 20mm and reaching 25m/s at 50mm.

5 Results - Discussion

5.1 High speed imaging

5.1.1 50Bar & 100Bar

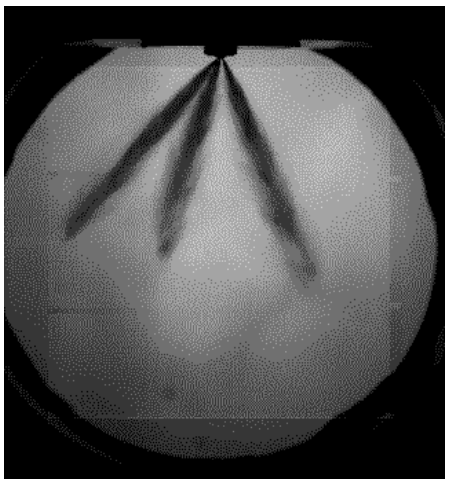

Figure 25: 50bar injection pressure, spray shape

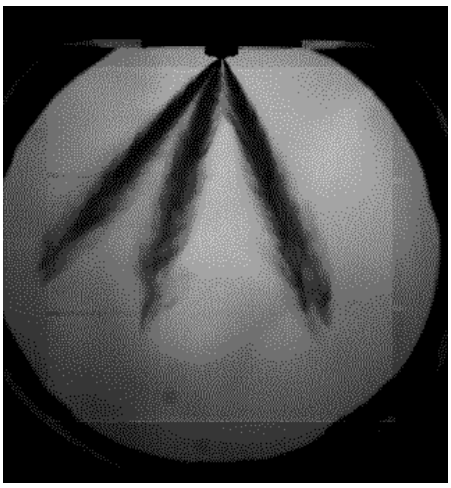

Figure 26: 100bar injection pressure, spray shape

5.1.2 150Bar & 200Bar

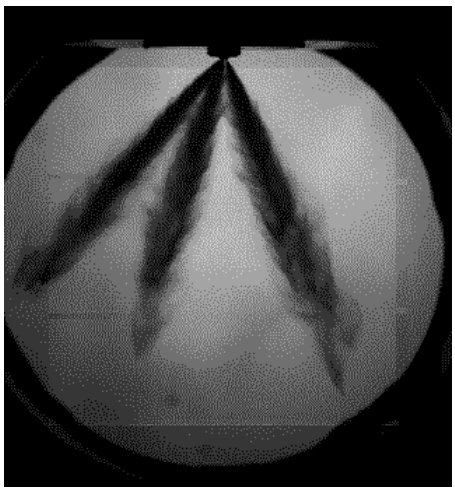

Figure 27: 200bar injection pressure, spray shape

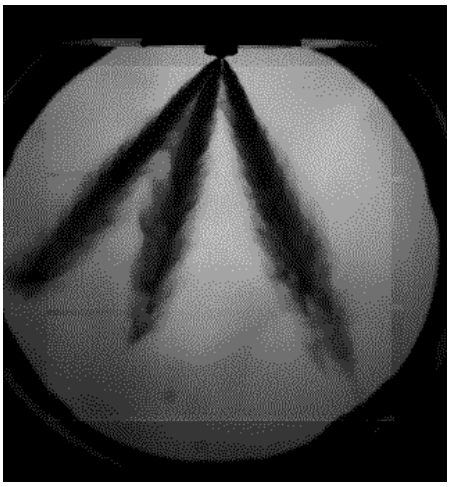

Figure 28: 150bar injection pressure, spray shape

From the high speed images it becomes clear that as the fuel pressure increases the spray penetration length increases as well, while the spray is more dense since more quantity of fuel is injected for a given injection duration. The increase of the injection pressure increases also slightly the overall spray angle while the shear stresses between the air and the fuel cause small vortices to appear as well.

5.2 Influence of fuel pressure

5.2.1 25Bar

At 25 bar injection pressure the velocity of the droplets is not high enough, reaching an average value of 24m/s, to create a clear time-versus-velocity spray pattern. From the six different measured positions the highest average velocity of 24,3 m/s is observed at the radial position of 28mm. The highest velocity droplets for this injection pressure reach values of 45m/s. Because the injection pressure is low and the fuel is injected into non vaporizing conditions, there is not a major droplet diameter difference between the spray core position and the other positions. The maximum D10 value is 17,3μm while the D32 value reaches 31,4μm and the spray core is identified at 26mm radial position.

The inconsistency regarding the spray core position between the velocity and the droplet diameter measurements can be attributed to the low injection pressure which creates a weak spray that is easily affected by cyclic variations and ambient conditions.

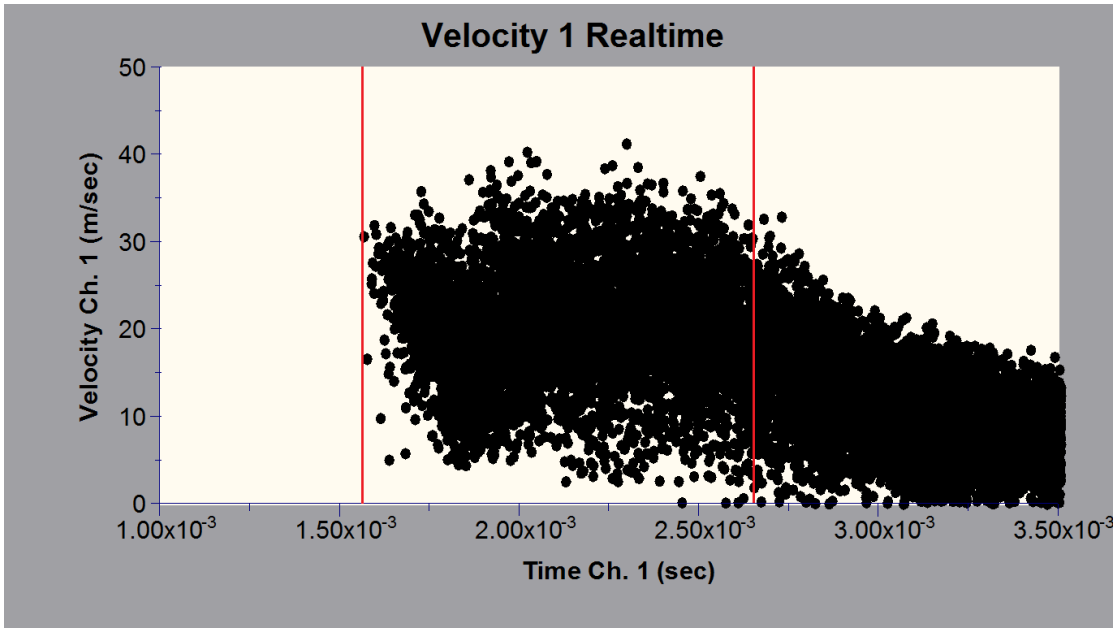

Figure 29: 25bar time-velocity diagram

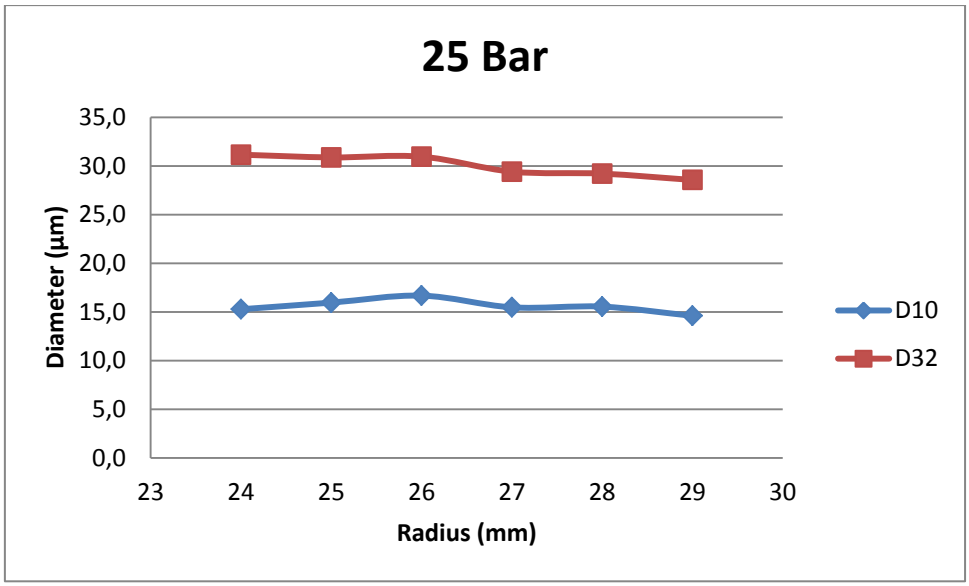

Figure 30: Droplet diameter for six radial positions, 25bar injection pressure

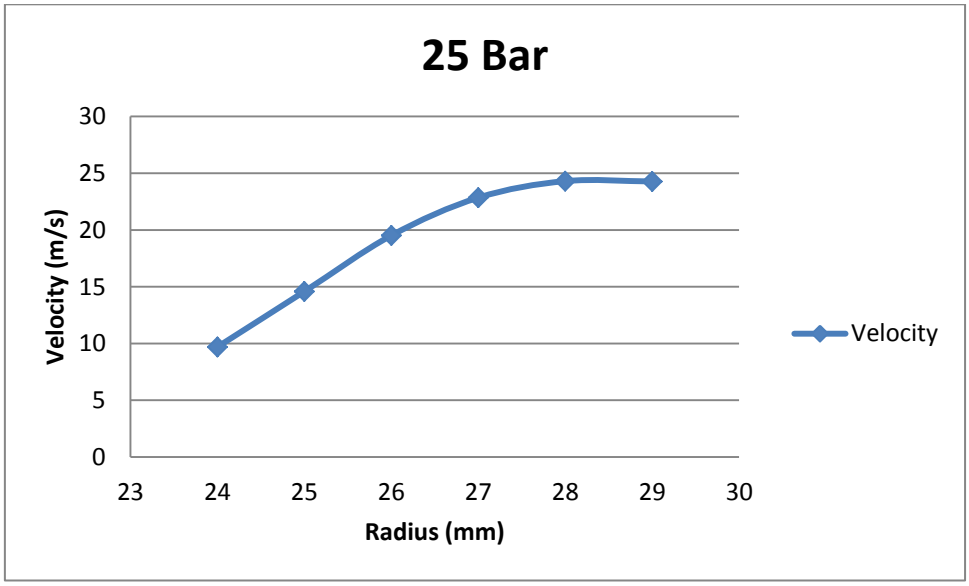

Figure 31: Droplet velocity for six radial positions, 25bar injection pressure

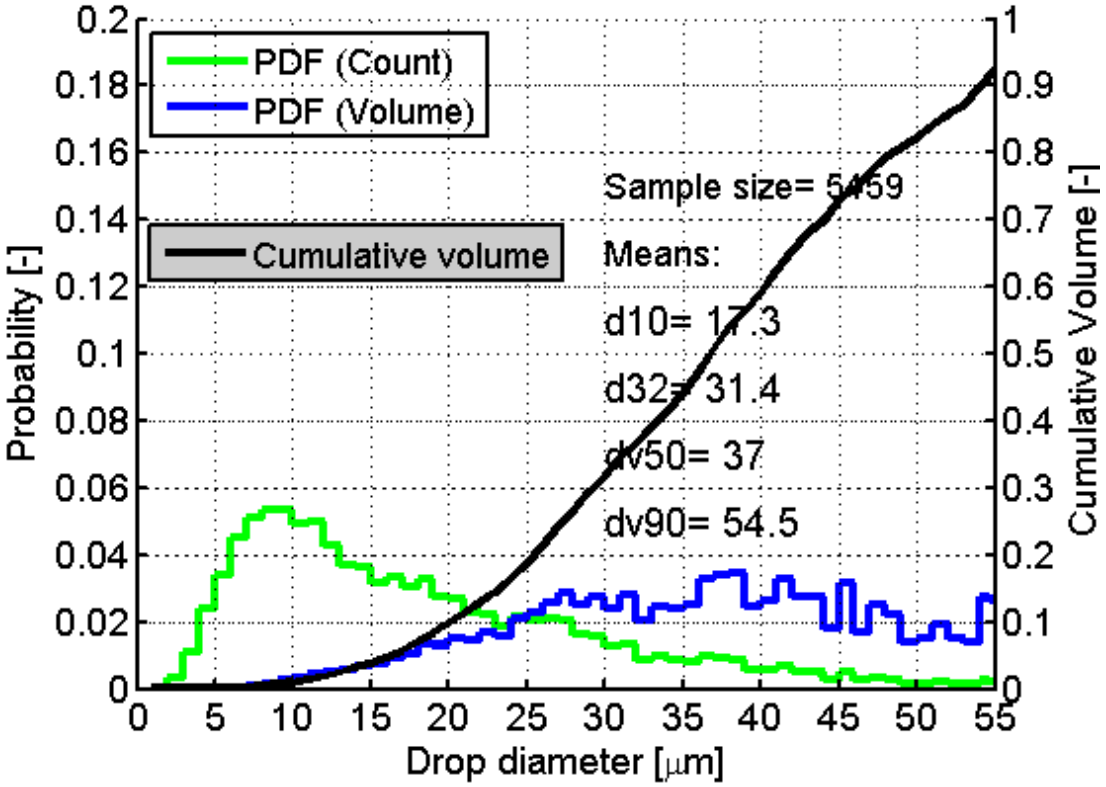

Figure 32: PDF graph and cumulative volume for 25bar injection pressure

5.2.2 50Bar

As the injection pressure increases to 50bar the time-versus-velocity graph of the spray becomes clearer. As a result a main injection part starts to become visible as well as a trailing part which appears after the injector closes. For the injection pressure of 50 bar the spray core position is identified at 28mm radial distance where the average velocity reaches 41m/s and the fastest droplets measured reach 60m/s. Regarding the droplet diameters, the increased pressure creates droplets with an average D10 of 16,3µm and a D32 of 25,9µm at the spray core position.

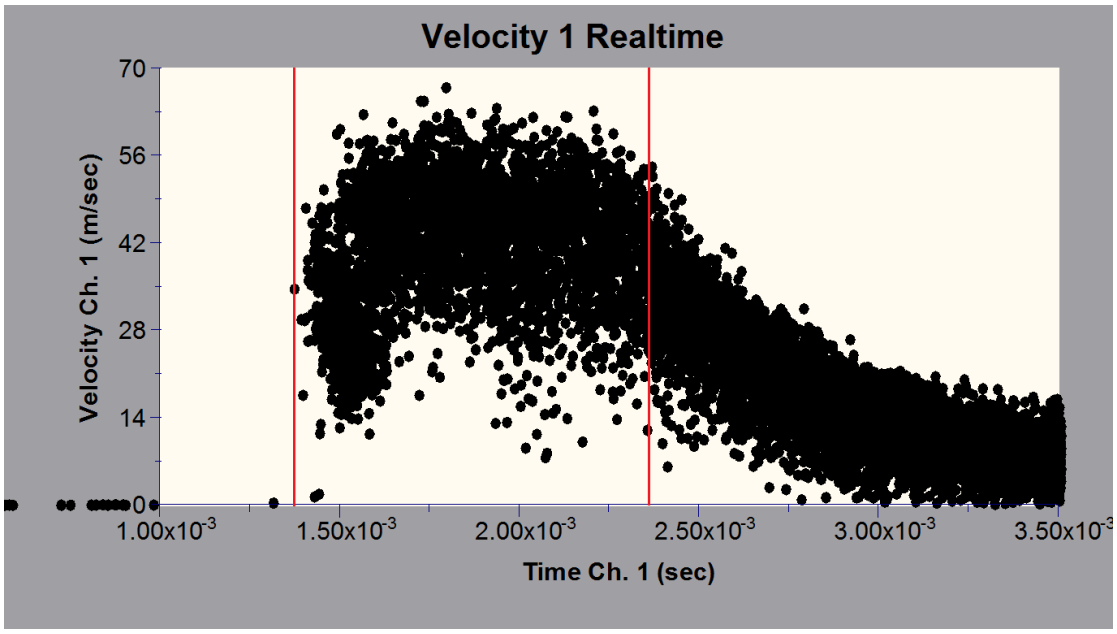

Figure 33: 50bar time-velocity diagram

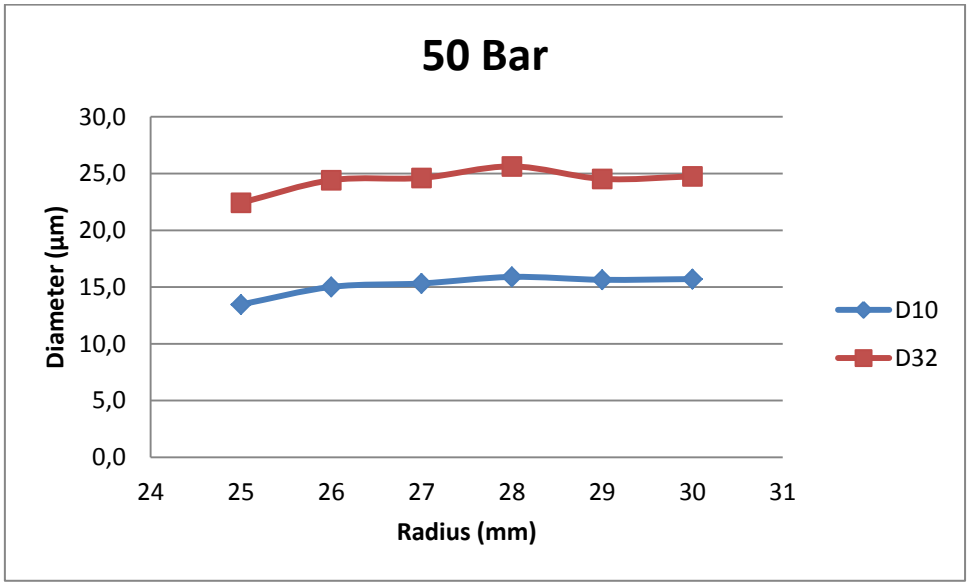

Figure 34: Droplet diameter for six radial positions, 50bar injection pressure

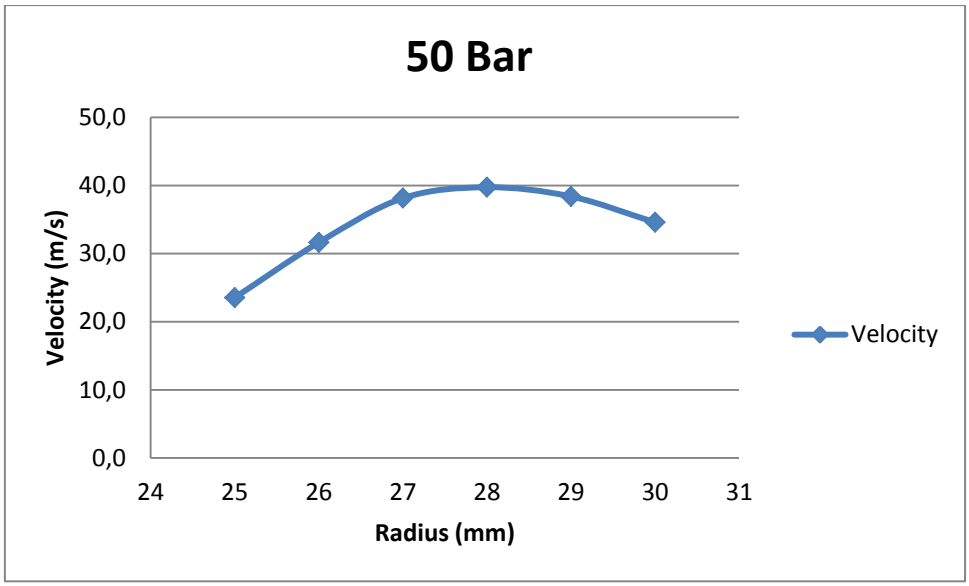

Figure 35: Droplet velocity for six radial positions, 50bar injection pressure

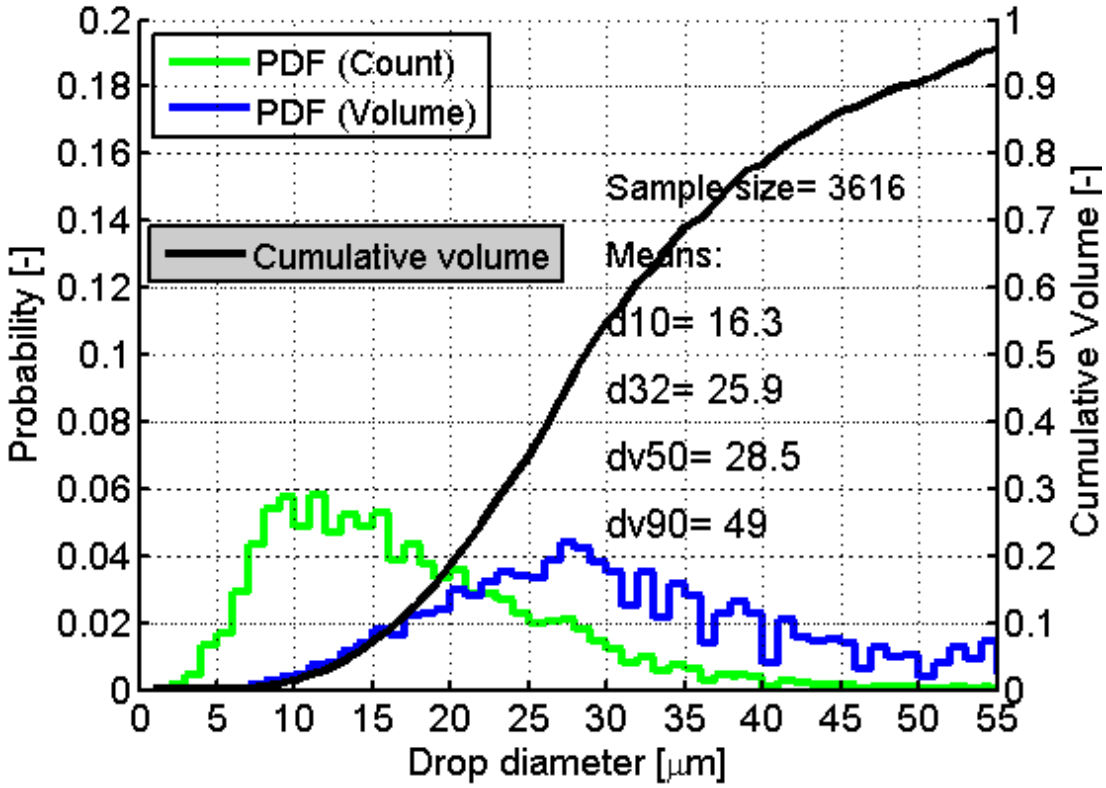

Figure 36: PDF graph and cumulative volume for 50bar injection pressure

5.2.3 100Bar

At 100bar injection pressure the spray shape is clearly distinguishable into two parts. The first part which appears during the actual injection event and is the most important in the injector performance analysis and the second part which consists of low velocity droplets that are created after the injector closes. The spray core is identified at 27mm radial distance from the injector nozzle and the average velocity at that point reaches 58,6m/s while the fastest droplets reach 85m/s. At that injection pressure the droplet diameters at the spray core reach a D10 value of 14,5μm and a D32 of 20,5μm.

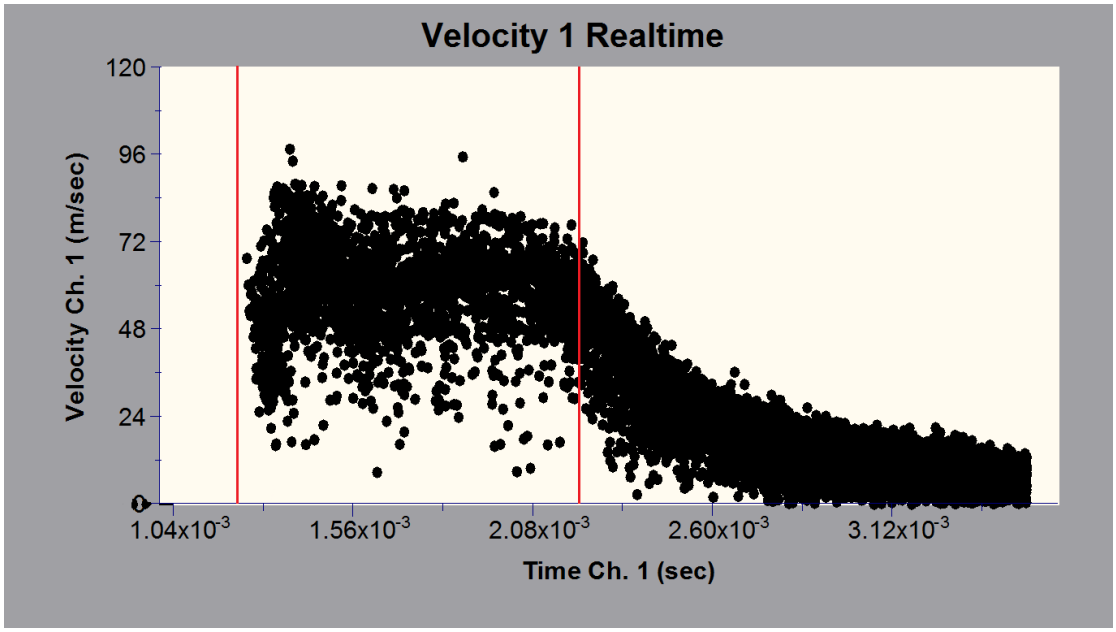

Figure 37: 100bar time-velocity diagram

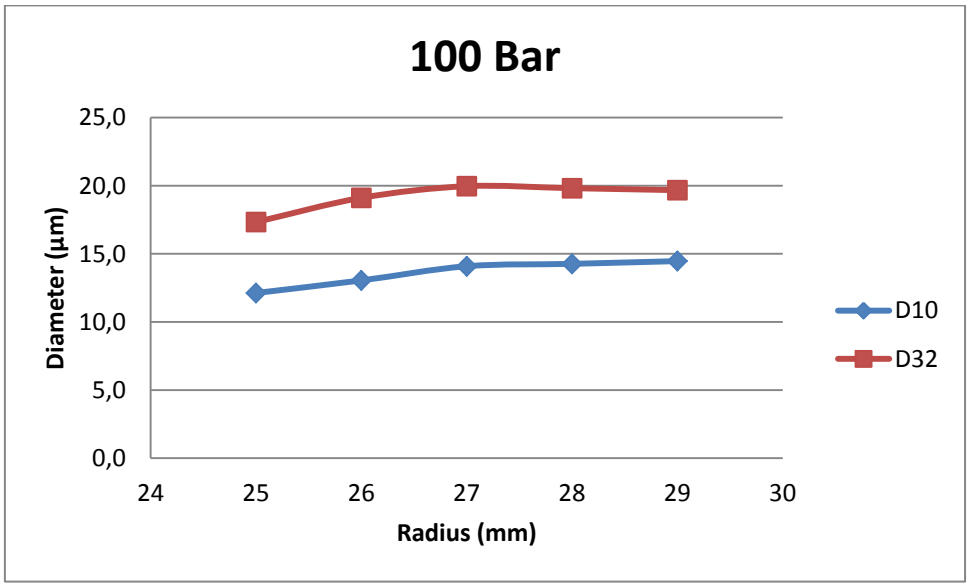

Figure 38: Droplet diameter for five radial positions, 100bar injection pressure

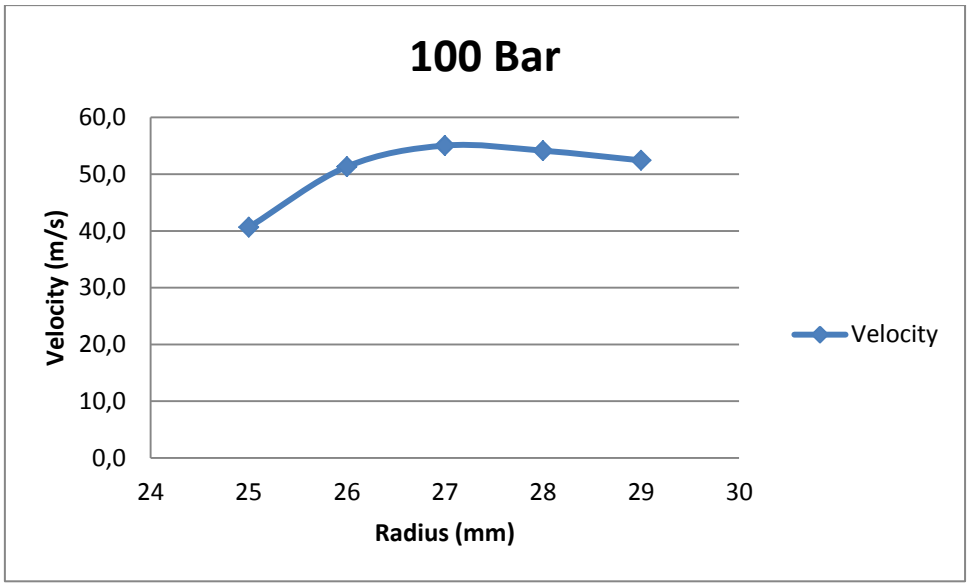

Figure 39: Droplet velocity for five radial positions, 100bar injection pressure

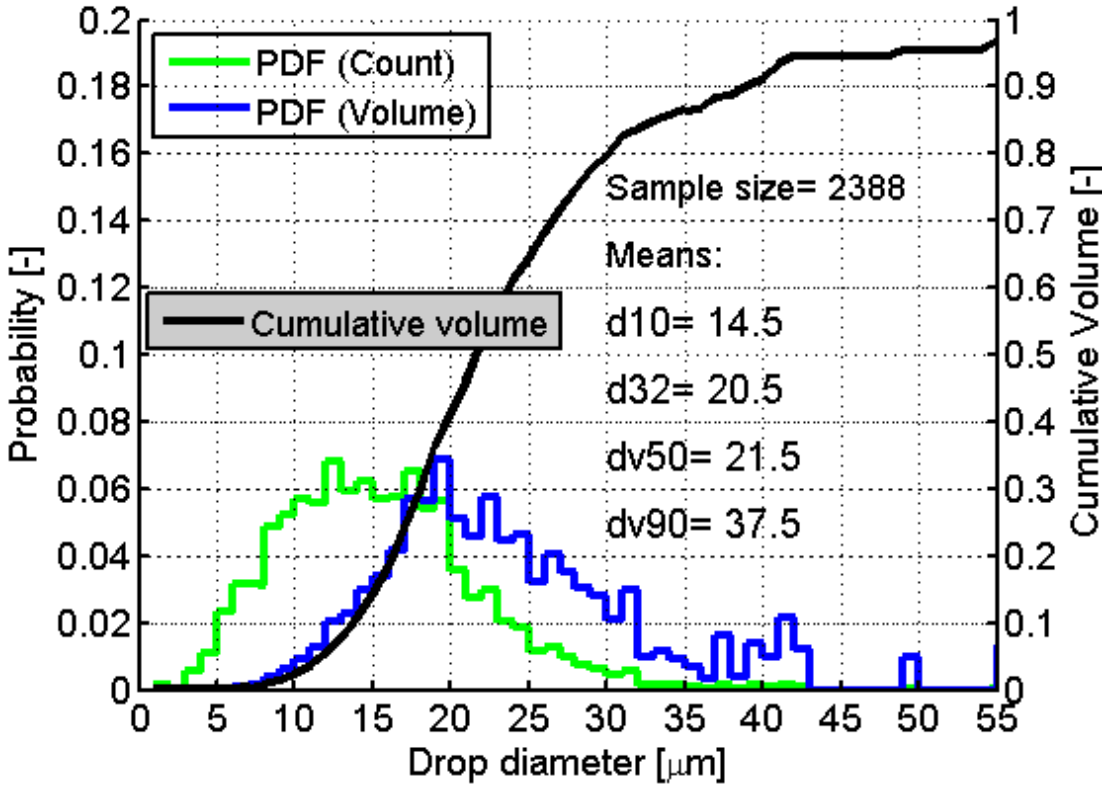

Figure 40: PDF graph and cumulative volume for 100bar injection pressure

5.2.4 150Bar

As the injection pressure increases it becomes more difficult for the phase Doppler system to acquire the injection data and that is obvious in the velocity versus time diagram where the main injection area becomes less dense for the same number of acquired droplets. Still it is possible to acquire enough validated data in order to have accurate results.

As the injection pressure increases the spay plume changes position and now the spray core is identified at 29mm radial distance from the injector tip. For the 150bar injection the D10 value reaches 13,9μm and the D32 is 19,2μm while the velocity is 58 m/s.

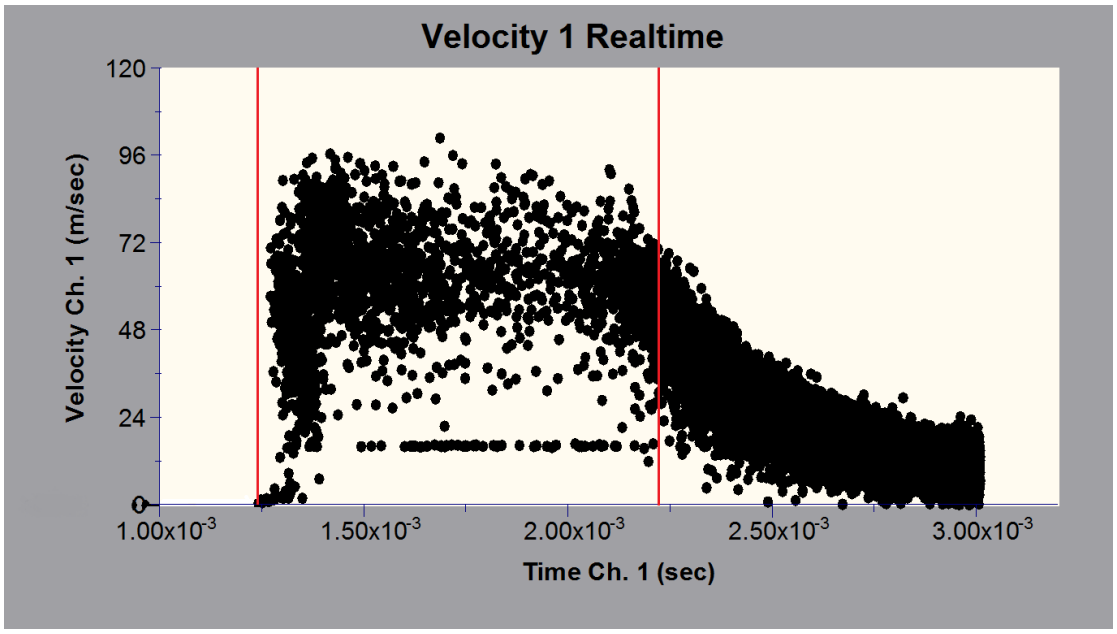

Figure 41: 150bar time-velocity diagram

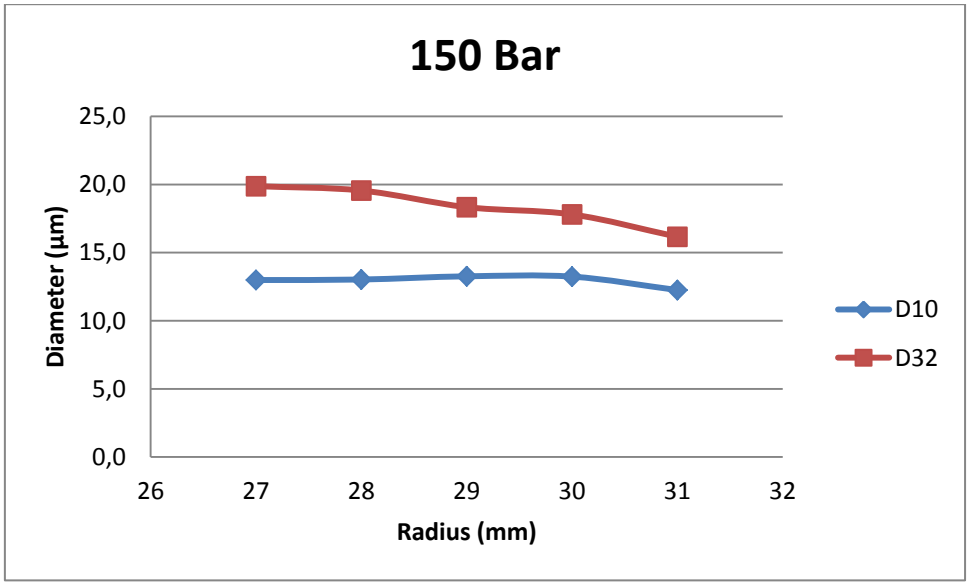

Figure 42: Droplet diameter for five radial positions, 150bar injection pressure

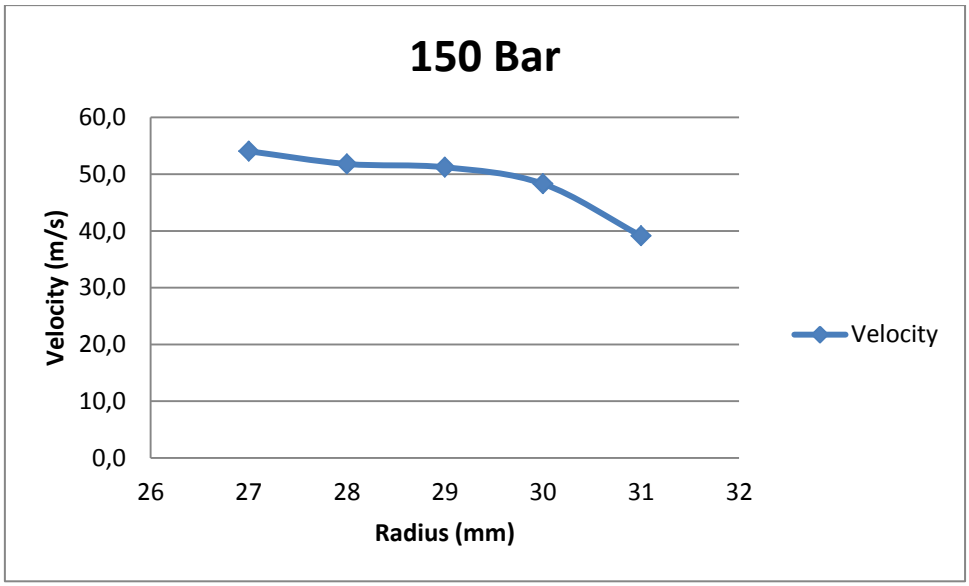

Figure 43: Droplet velocity for five radial positions, 150bar injection pressure

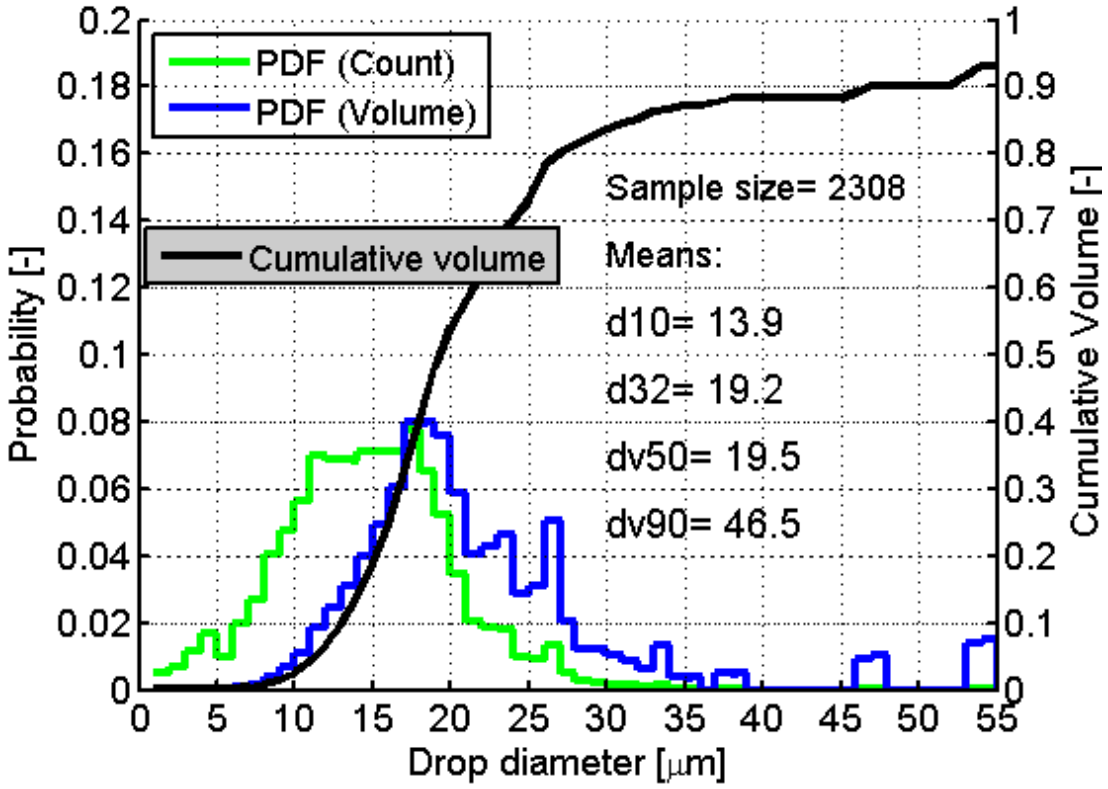

Figure 44: PDF graph and cumulative volume for 150bar injection pressure

5.2.5 200Bar

The remarks that were true for the 150bar injection pressure, apply also to the 200bar injection pressure. The high injection pressure makes the data acquisition even more difficult and time demanding. The highest velocity droplets that are captured reach 100m/s and the diameters reach a D10 of 12,4µm and a D32 of 18,4µm at the spray core position which is identified at 29mm radial distance from the injector nozzle.

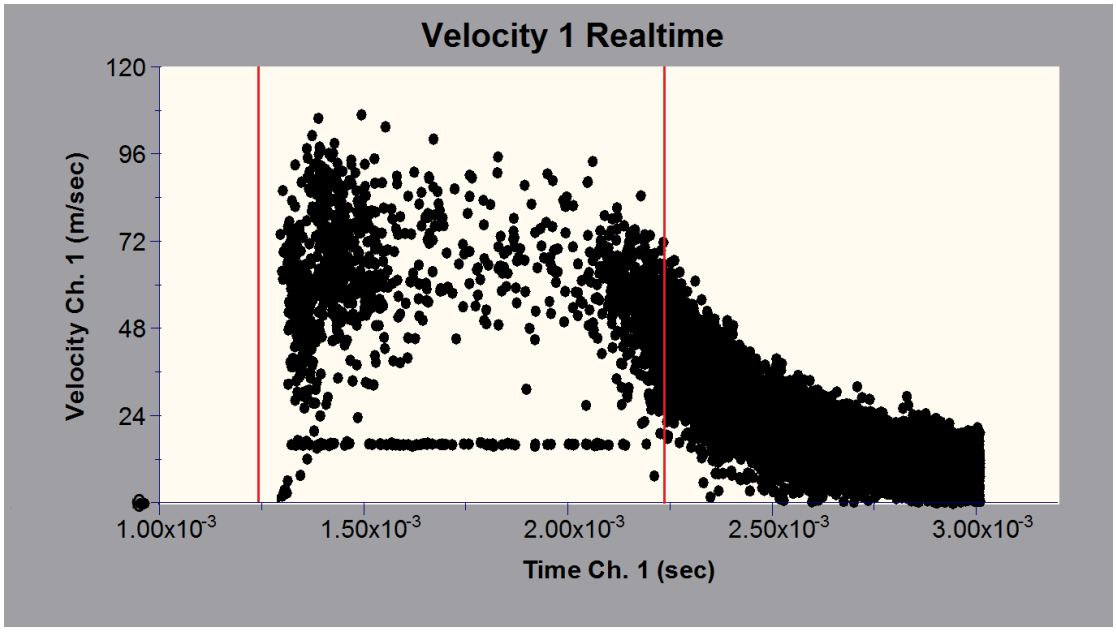

Figure 45: 200bar time-velocity diagram

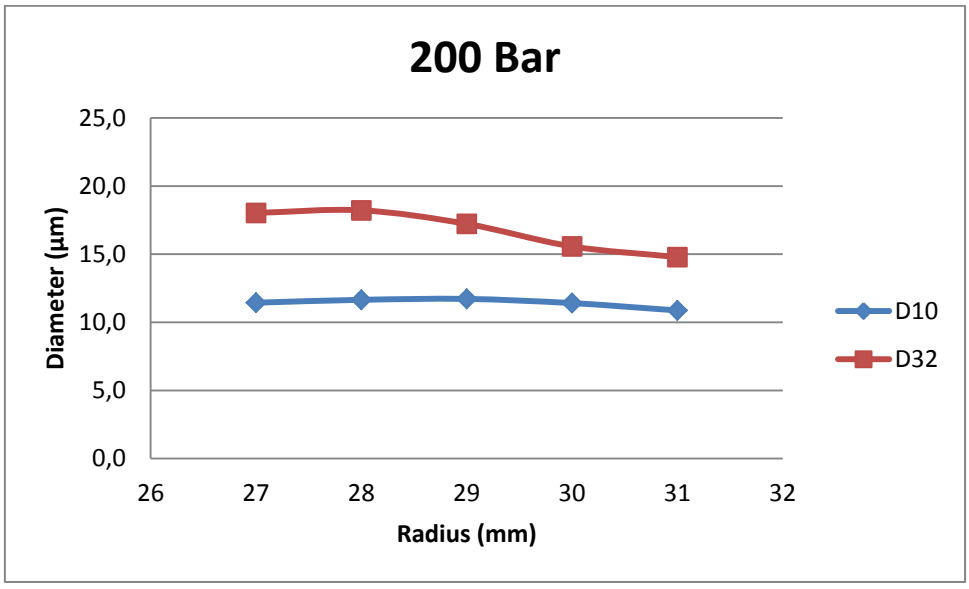

Figure 46: Droplet diameter for five radial positions, 200bar injection pressure

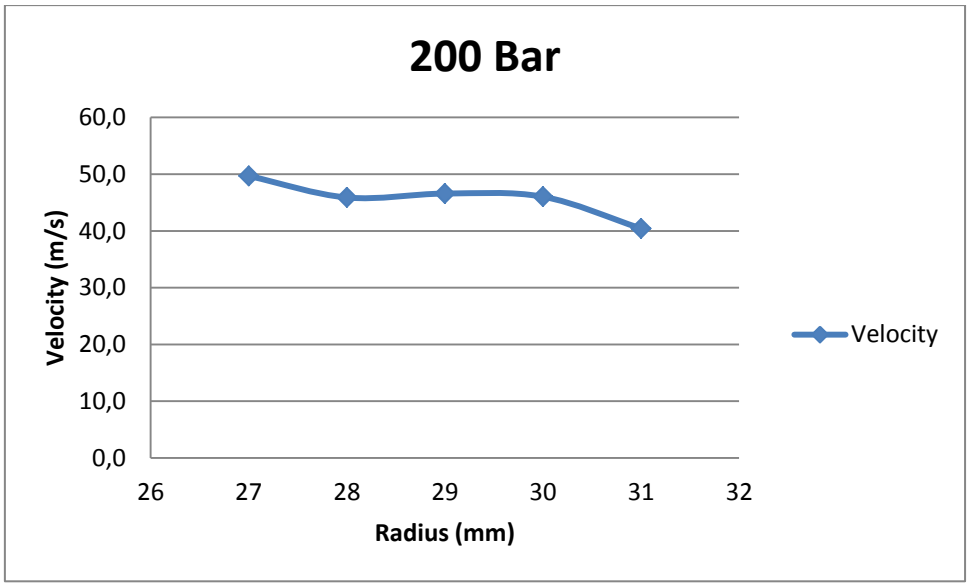

Figure 47: Droplet velocity for five radial positions, 200bar injection pressure

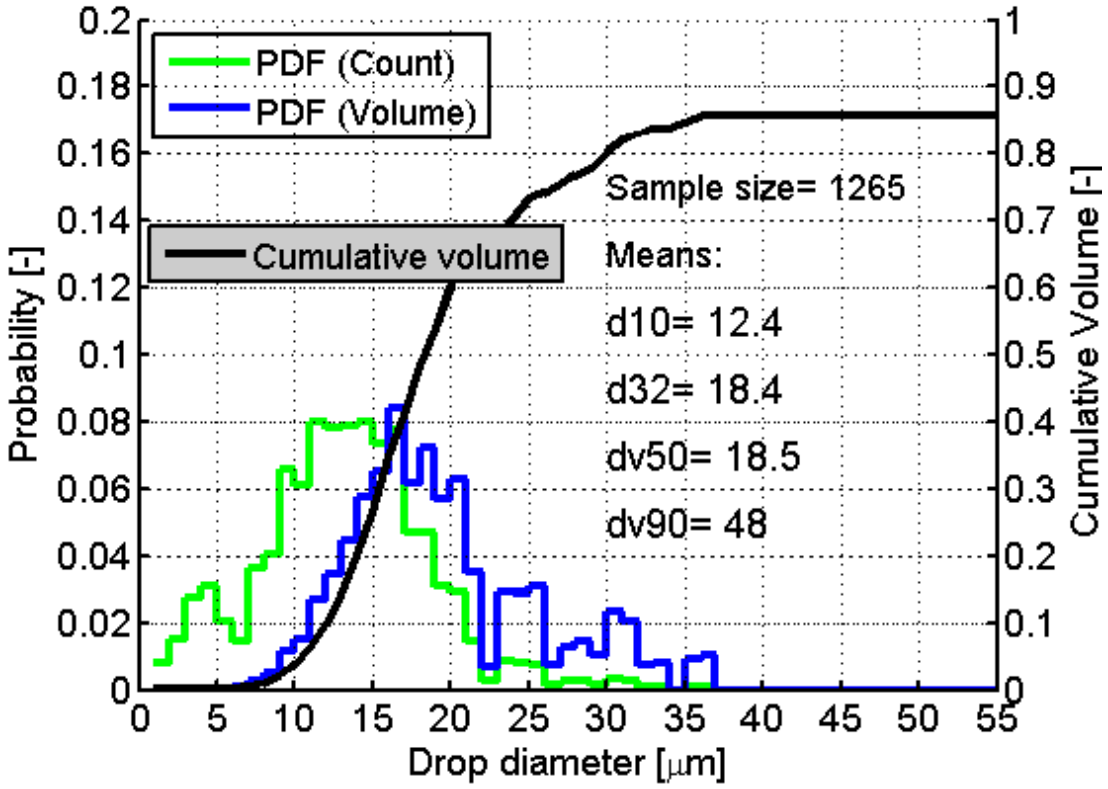

Figure 48: PDF graph and cumulative volume for 200bar injection pressure

5.2.6 Overall comparison of pressure influence

From the results it becomes clear that as the injection pressure increases the droplet diameter, both D10 and D32 decrease. The D32 values exhibit the highest influence from the injection pressure since the value decreases from the 31,4μm at 25bar injection pressure, down to 18,4μm at 200bar injection pressure. The D10 value decreases from 17,3μm down to 12,4μm. The decrease of both the D10 and D32 diameter with the increase of the injection pressure corresponds to a typical behavior of a multihole injector (Dahlander & Denbratt, 2005) and if the pressure could increase even more it would reach an asymptote at around 12,0μm (D10).

An interesting trend is observed when the results for the droplet velocities are plotted versus the injection pressure. As the pressure increases the velocity increases as well but reaches its maximum value of 58m/s at the 100bar injection pressure and afterwards does not increase anymore having the same value of 58m/s at 200bar. Literature suggests that as the injection pressure increases the droplet velocity increases as a square root function.

In our case, that does not happen. It is difficult to explain why this happens, since the exact validation routines that are used by the system to verify that the measurement is valid are not available to us and therefore cannot predict why higher speed droplets that appear in the measurements are rejected.

From the droplet distribution diagram it becomes clearer that the increased injection pressure reduces the droplet diameter and furthermore limits the range of diameters that droplets appears. For the injection pressures of 150 and 200bar the values over 20μm have less than 1% probability which is desirable because high diameter droplets have a large volume of fuel that can be difficult to evaporate fast enough. Finally it is worth noting that for all the different injection pressures the first droplets appear at least 1,2ms after the trigger signal. This corresponds to the 0,7ms delay between the injection signal and the injector tip opening, that is characteristic of a multihole injector, and the time required for the droplets to reach the measuring volume 30mm downstream the injector tip.

Table 4: Influence of fuel pressure on droplet diameter, spray core position

Injection Pressure (Bar)	D10 (µm)	D32 (µm)
25	17,3	31,4
50	16,3	25,9
100	14,5	20,5
150	13,9	19,2
200	12,4	18,4

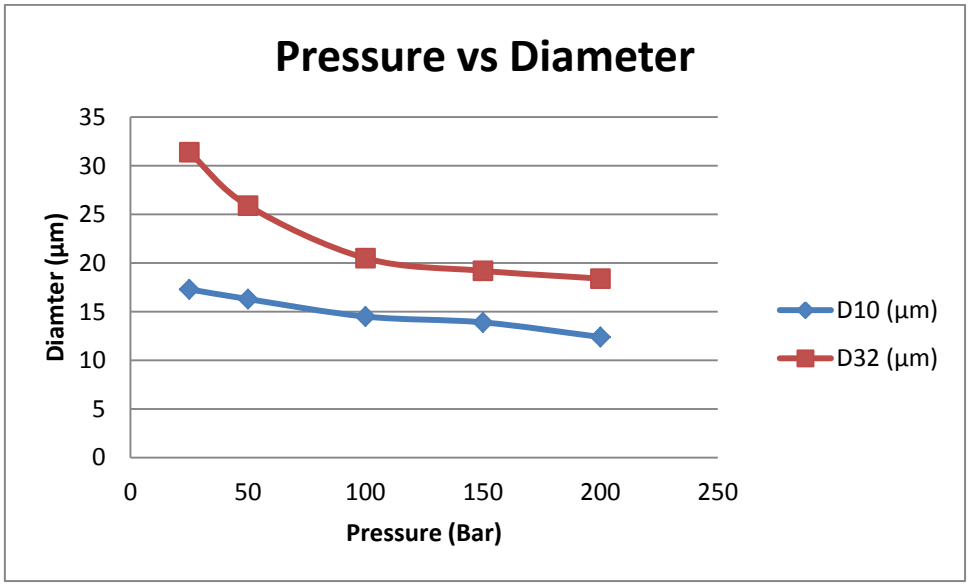

Figure 49: Influence of fuel pressure on droplet diameter

Table 5: Influence of fuel pressure on droplet velocity, spray core position

Injection Pressure (Bar)	Velocity (m/s)
25	20,1
50	41,0
100	58,6
150	58,0
200	58,1

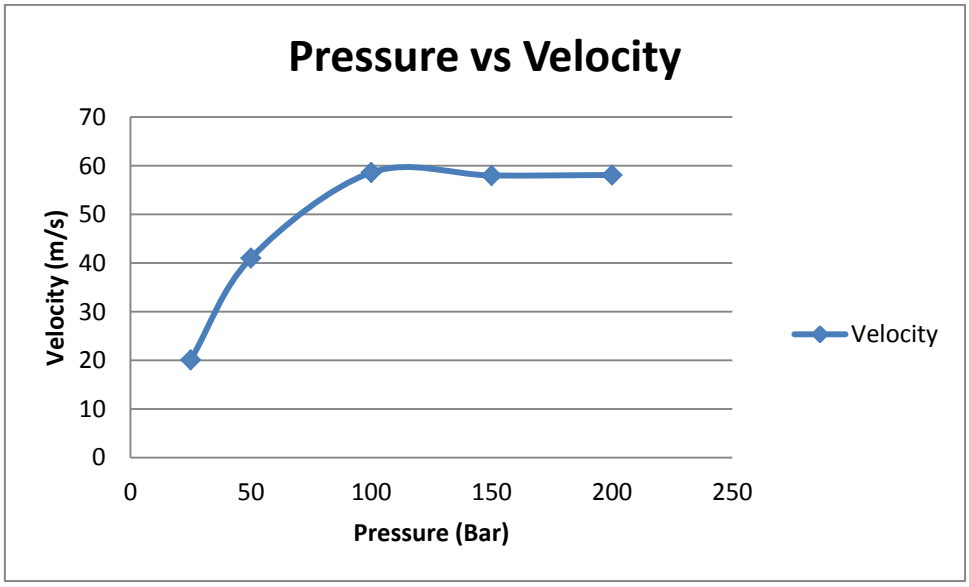

Figure 50: Influence of fuel pressure on droplet velocity

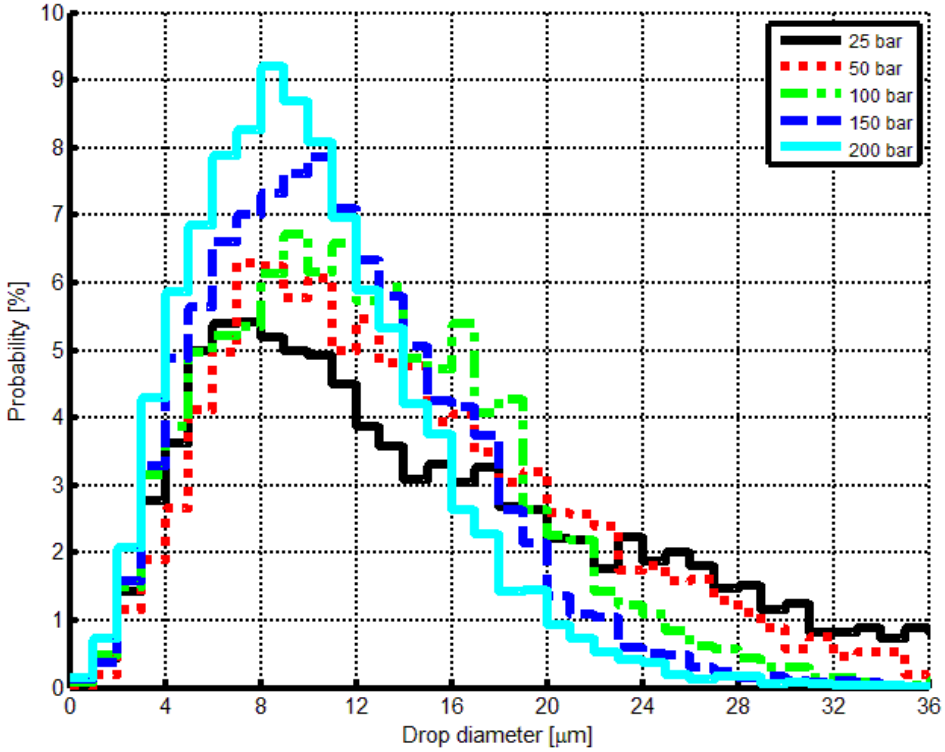

Figure 51: PDF graph, droplet diameters for five different fuel pressures

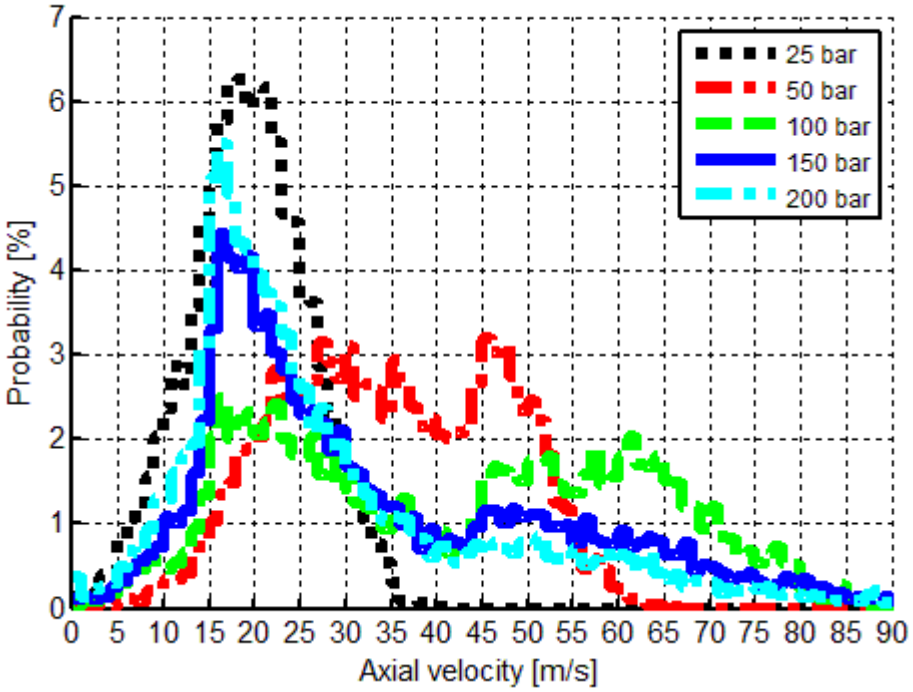

Figure 52: PDF graph, droplet velocity for five different fuel pressures

5.3 Influence of injection duration with constant pressure

5.3.1 1.5ms

The minimum injection duration that was tested was 1,5ms and was considered the base measurement from which the different injection durations are going to be compared. The following results are the same as the results of the 100bar injection pressure from the previous measurements.

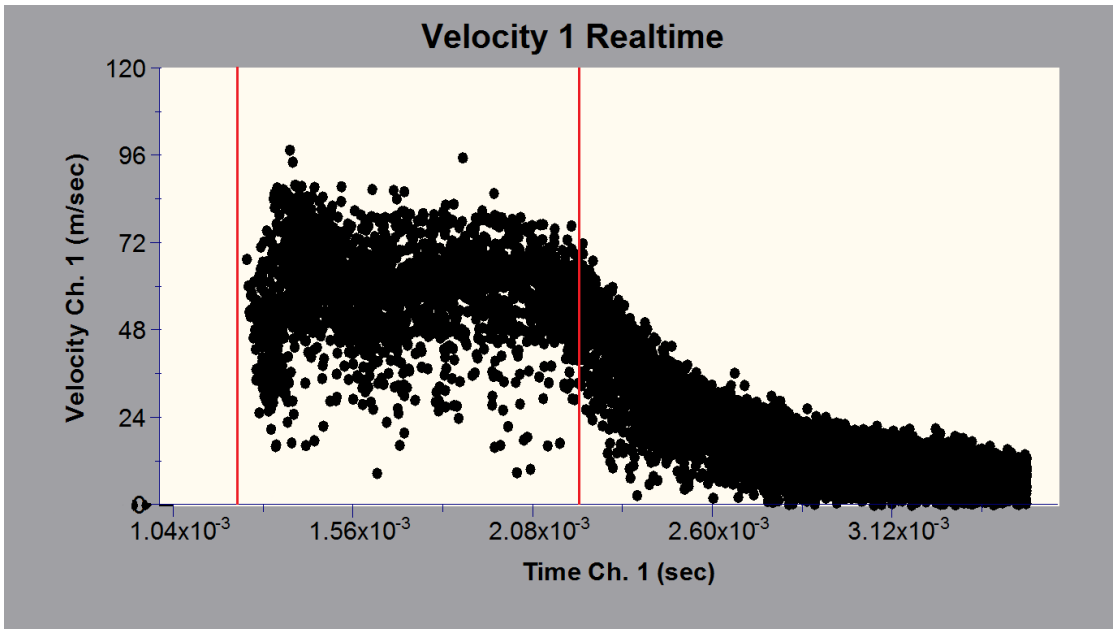

Figure 53: Time-velocity diagram, 1.5ms injection duration

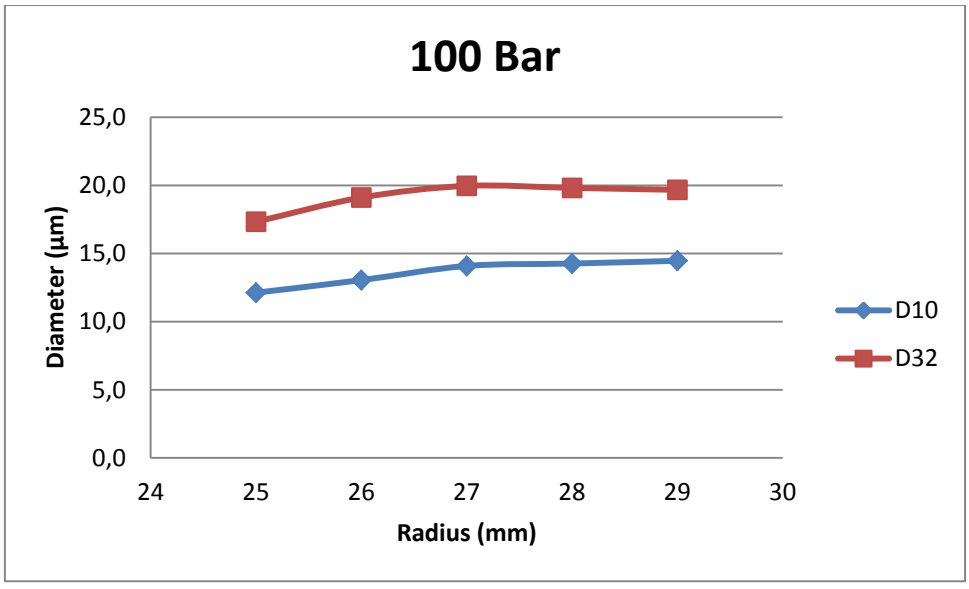

Figure 54: Droplet diameter for five radial positions, 1.5ms injection duration

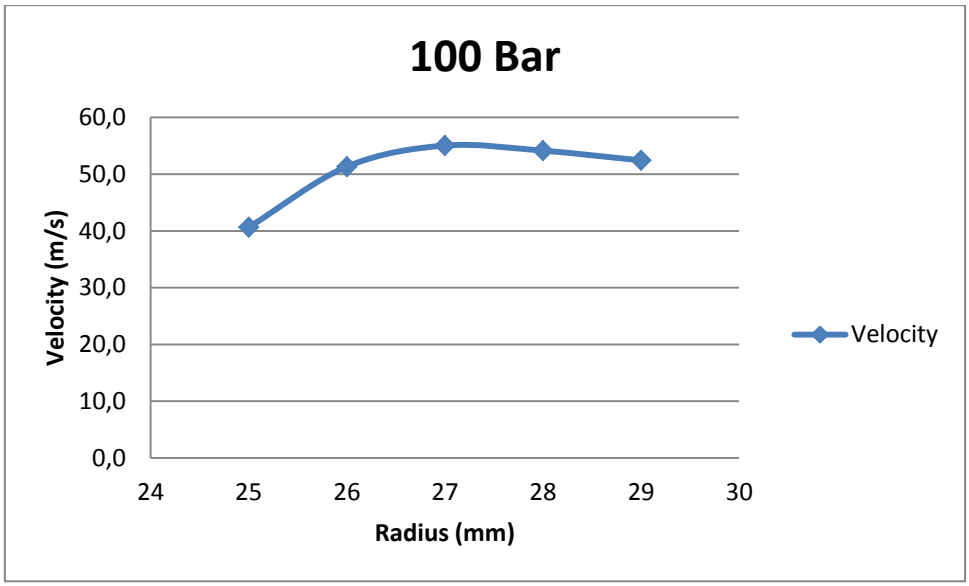

Figure 55: Droplet diameter for five radial positions, 1.5ms injection duration

5.3.2 3.0ms

As the injection duration is increased to 3ms, double the duration of the base measurement, the two different parts that form the spray become even more clear. During the first part, while the injector is open, medium to high velocity droplets of varying diameter appear, whereas when the injector closes the velocity decreases rapidly and medium to low diameter droplets are created. During the important phase, while the injector is open, at the spray core position, which is at 27mm radial distance from the injector tip, the average velocity is 59,6m/s and the fastest droplets reach velocities of around 85m/s. The diameters at the spray core have a D10 value of 14,7µm and a D32 of 19,9µm.

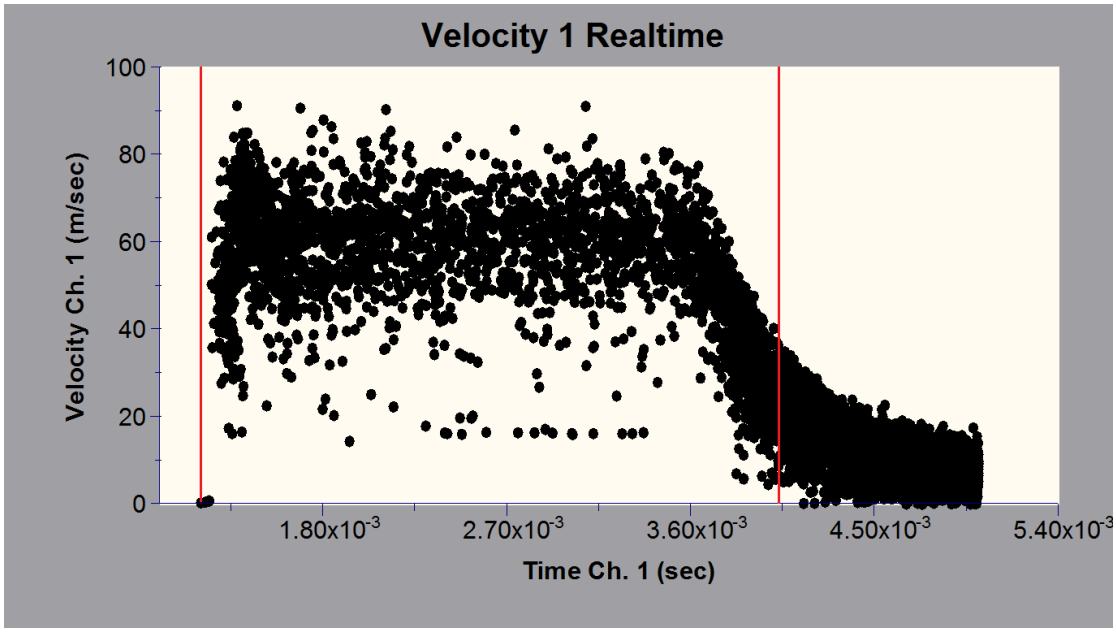

Figure 56: Time-velocity diagram, 3.0ms injection duration

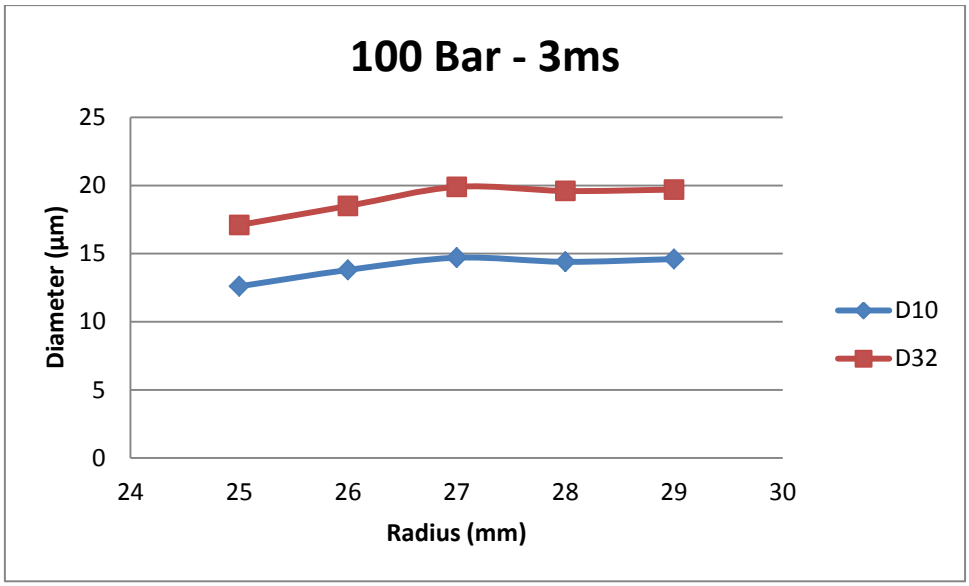

Figure 57: Droplet diameter for five radial positions, 3.0ms injection duration

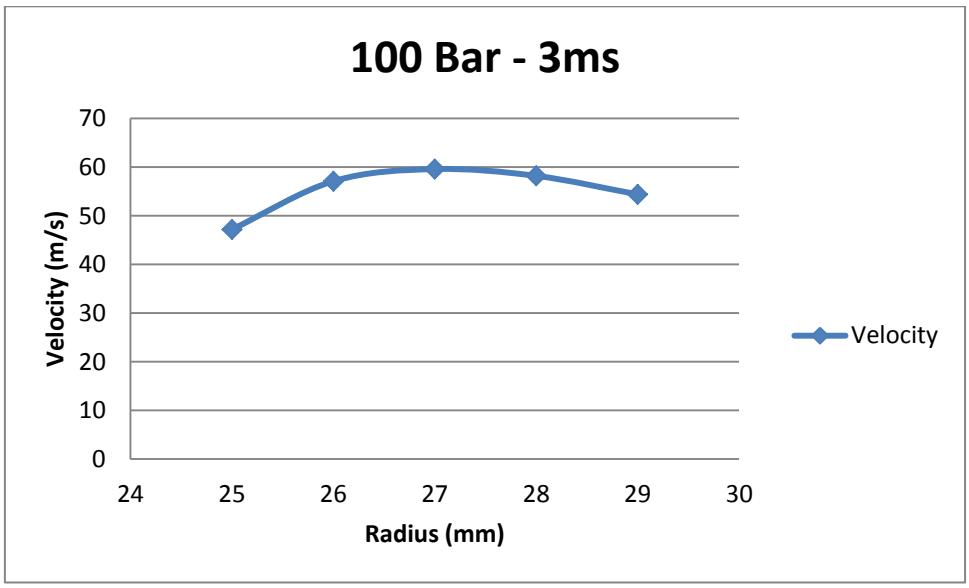

Figure 58: Droplet velocity for five radial positions, 3.0ms injection duration

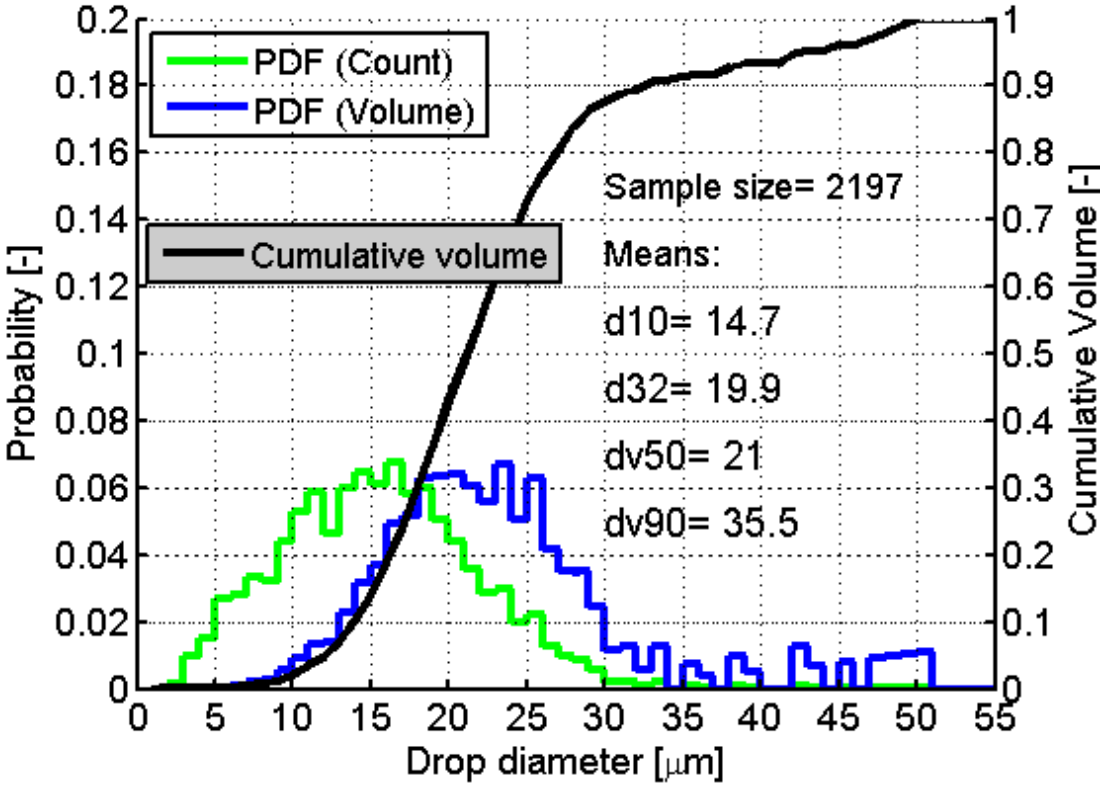

Figure 59: PDF graph and cumulative volume for 3.0ms injection duration

5.3.3 5.0ms

The last case of different injection duration is the 5ms case. The time-versus-velocity diagram does not have any significant difference compared to the 3ms case, it looks as an extended 3ms diagram. The spray core remains at the same radial position of 27mm but because of the non-vaporizing conditions and the high injection duration there is little variation in the droplet diameters between each measuring position. Nevertheless at the spray core position the D10 value is 14,4µm and the D32 is 19,4µm. The average velocity is 58,4m/s while the fastest droplets reach velocities of up to 87m/s.

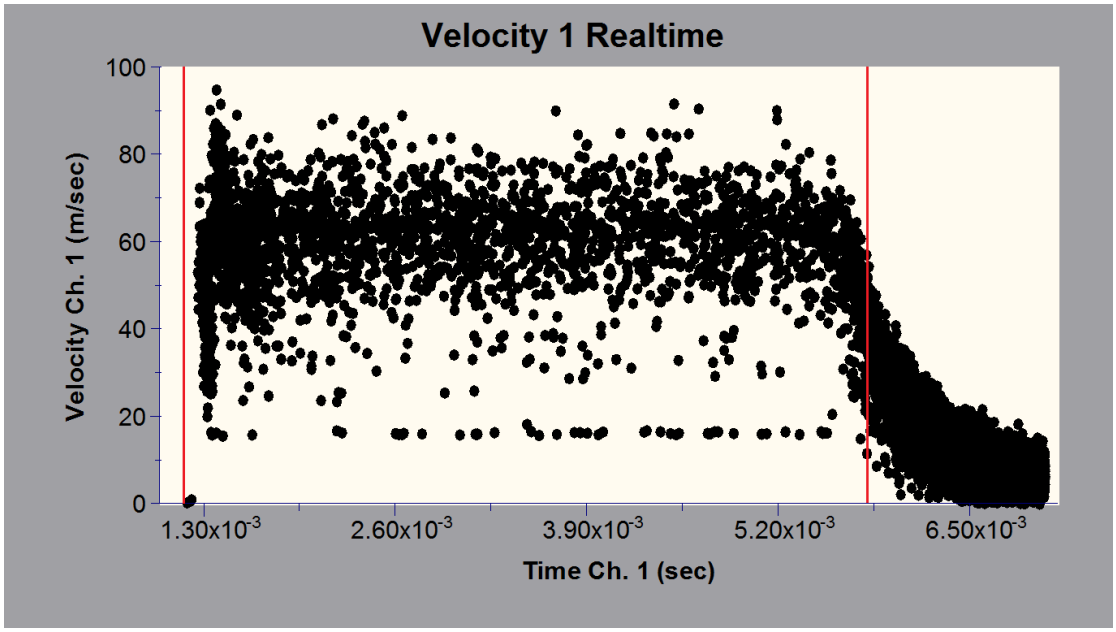

Figure 60: Time-velocity diagram, 5.0ms injection duration

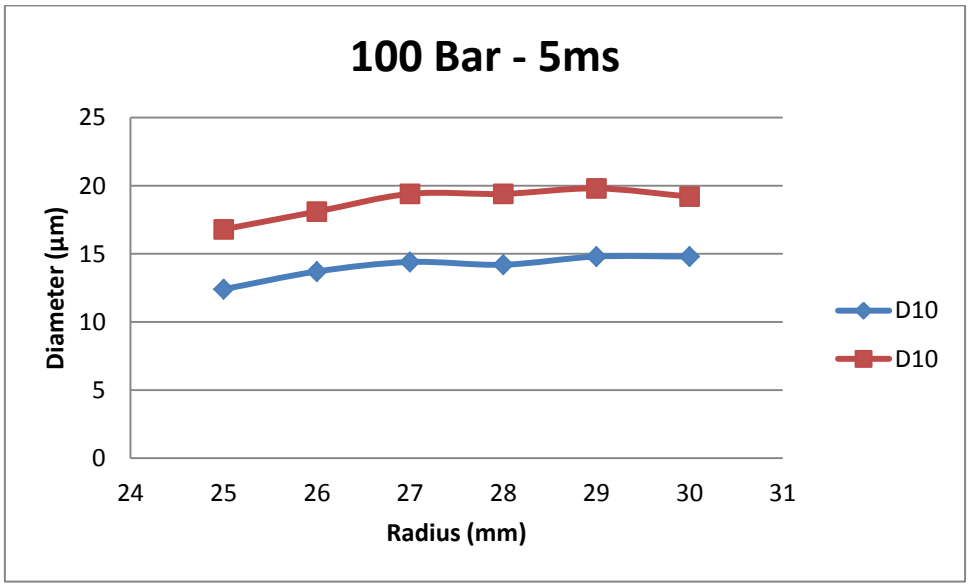

Figure 61: Droplet diameter for five radial positions, 5.0ms injection duration

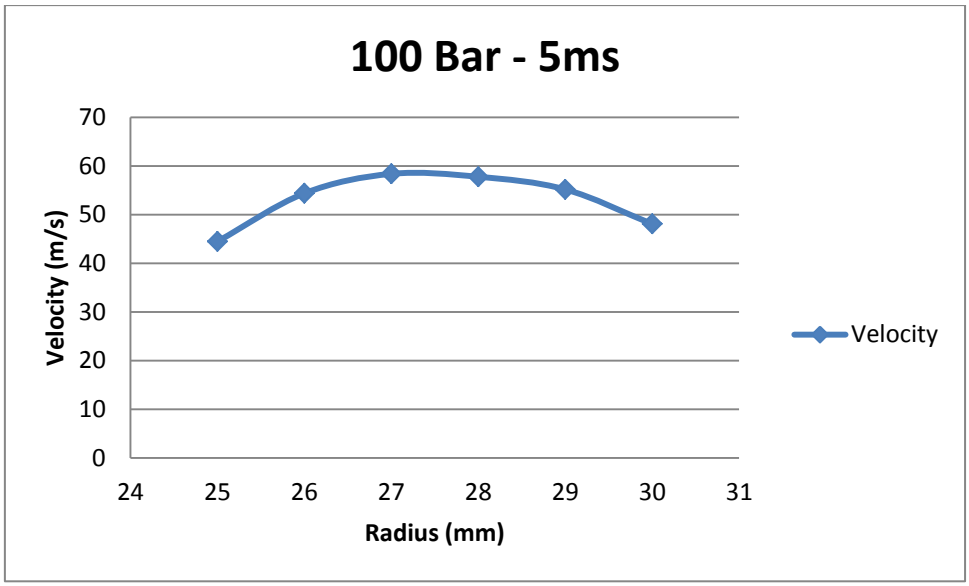

Figure 62: Droplet velocity for five radial positions, 5.0ms injection duration

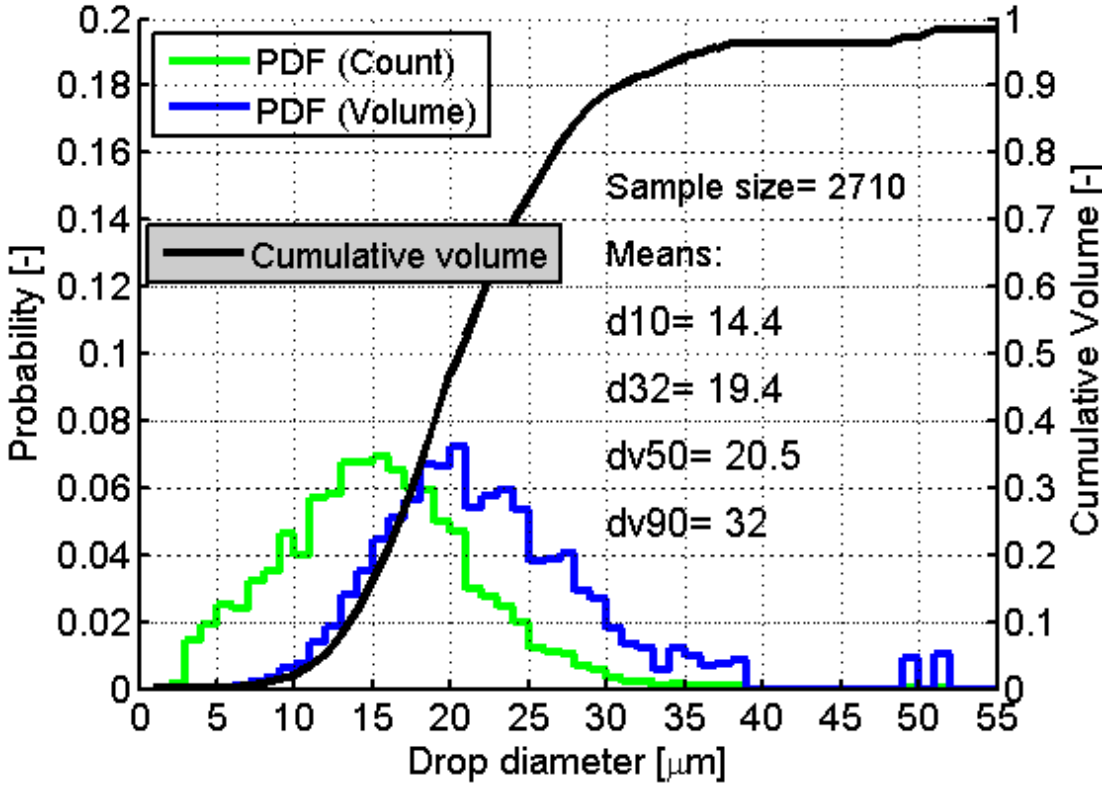

Figure 63: PDF graph and cumulative volume for 5.0ms injection duration

5.3.4 Overall comparison of the influence of injection duration

In order to get a better overview of the differences between the different injection duration on droplet velocities and diameters, while keeping the pressure constant, it is necessary to plot the results from the spray core position side by side. It is obvious that as the injection duration is increased there is a small change in the droplet diameter and droplet velocity. The D32 value decreases slightly for the 3ms injection duration and reaches a decrease of 5% for the 5ms injection duration. The D10 diameter remains almost the same for the 3ms injection duration, D10 of 14,7μm compared to the D10 of 14,5μm for the 1,5ms duration, while the D10 for the 5ms injection duration has a D10 of 14,4μm. Regarding the droplet velocities, the differences between each injection duration are lower than 1m/s, meaning that the velocity is not affected from the increased duration.

Table 6: Influence of injection duration on droplet diameter and velocity, spray core position, 100bar injection pressure

Inj. Duration (ms)	D10 (μm)	D32 (μm)	Velocity (m/s)
1,5	14,5	20,5	58,6
3	14,7	19,9	59,6
5	14,4	19,4	58,4

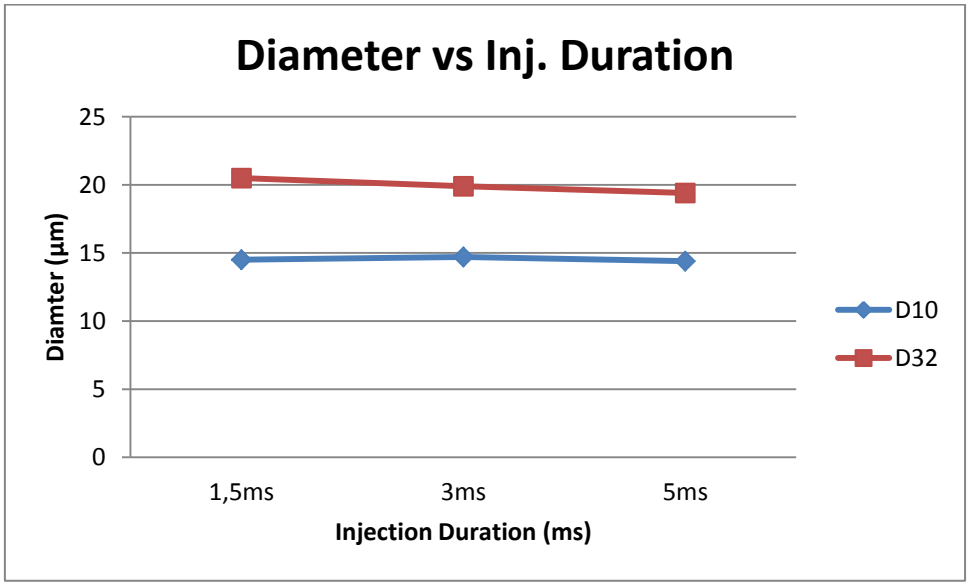

Figure 64: Droplet diameter variance for three different injection duration

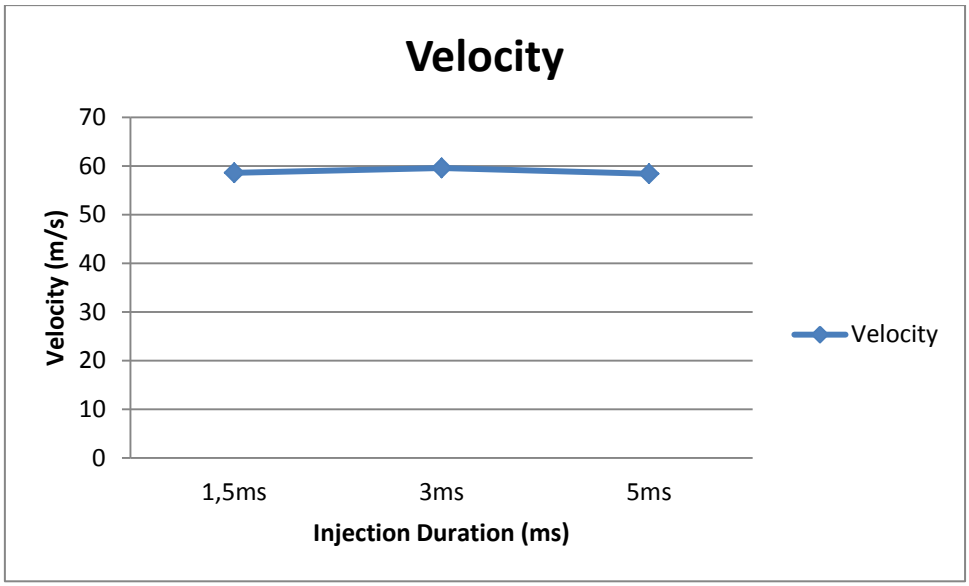

Figure 65: Droplet velocity variation for three different injection duration

5.3.5 Droplet & velocity distribution

Although it might seem that the injector performs quite different as the injection duration increases, it is important to compare not just the average values but the whole droplet diameter distribution and velocity distribution in a probability density function diagram. It is clear that while there are minor differences the plots are very similar, meaning that for the three different cases the injector performs almost the same. The same observation can be said also when observing the velocity diagram where the plots are almost equal except for velocities between 60m/s and 70m/s where the 5ms injection duration appears to create faster droplets.

Regarding the fact that the probability density plots are almost equal, it can be said that since the injector needle is completely open in all three cases the highest influence comes from the injection pressure rather than the duration of the injection. Some further investigation is necessary in order to determine the reason that the 5ms injection duration gives slightly smaller droplets and lower velocities, but a first suggestion can be attributed to the pressure waves inside the injector and the fuel rail. As the injector opens a negative pressure wave propagates through the fuel rail. When the wave reaches the fuel pump is reflected as a positive pressure wave. If that wave reaches the injector nozzle while the injector is open, it can increase the injection pressure, enough so as to create smaller diameter droplets.

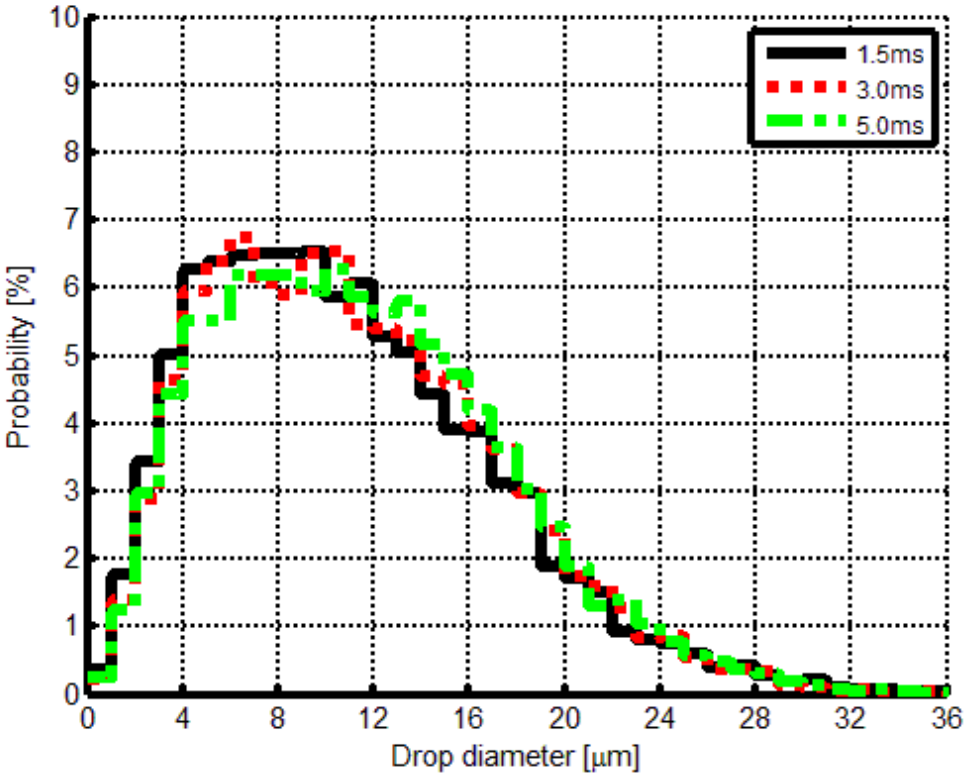

Figure 66: : PDF graph, droplet diameters for three different injection pressures

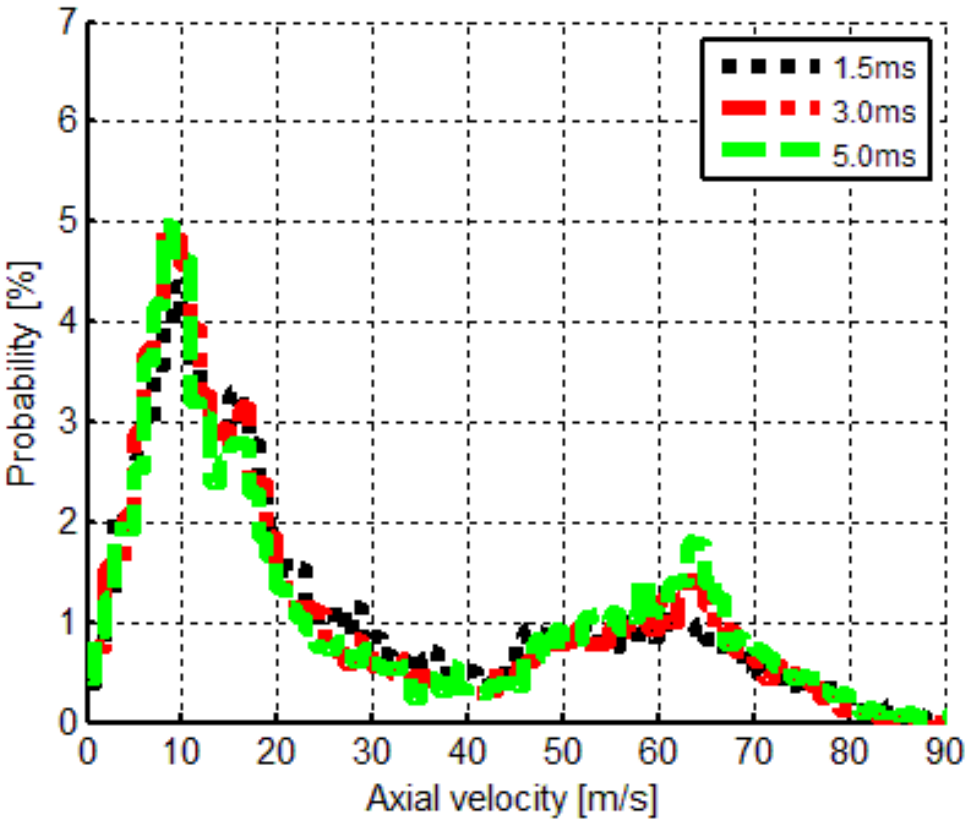

Figure 67: PDF graph, droplet velocity for three different injection pressures

5.4 Influence of double injection

The final approach tested was the ability of the injector to perform multiple injection events, more specifically double injection. Furthermore if the double injection was possible it was necessary to find the minimum time interval between each injection. Again the baseline which was used was the 100bar single injection. In order to get more accurate results each injection event from the double injection was processed as a single injection.

5.4.1 Single Injection

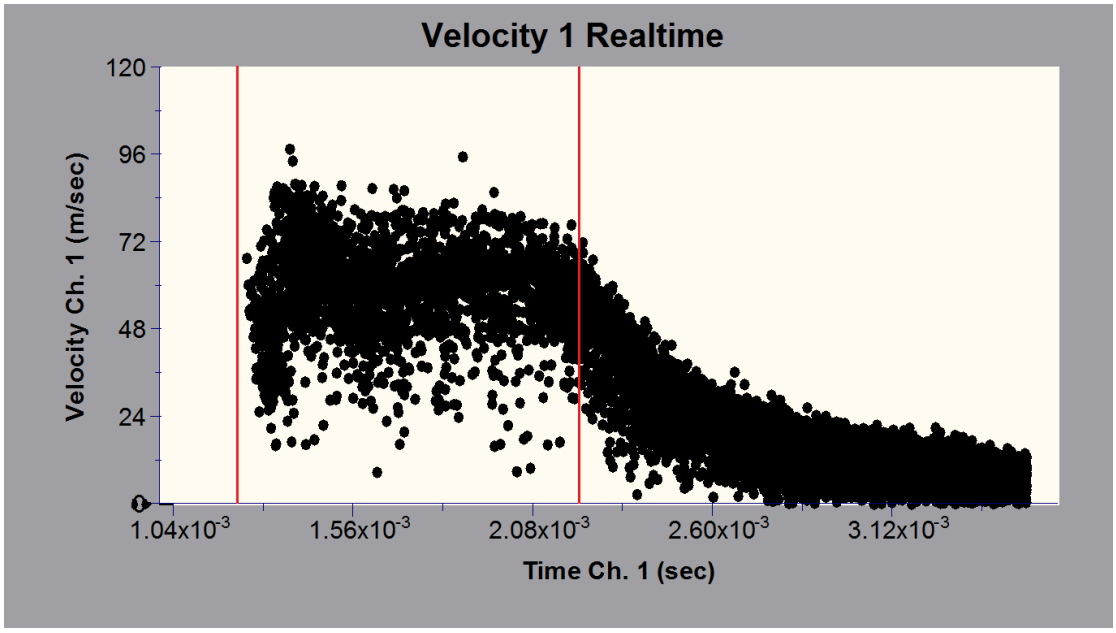

Figure 68: Time-velocity diagram, single injection

5.4.2 Double Injection

From the results it is obvious that the specific injector can perform a double injection. The minimum time interval between each injection was found to be 0,3ms. Below that value without further investigation is unclear whether the injector performs two injections but the different plumes merge or that the injector is incapable of following the injection signal and performs a single injection.

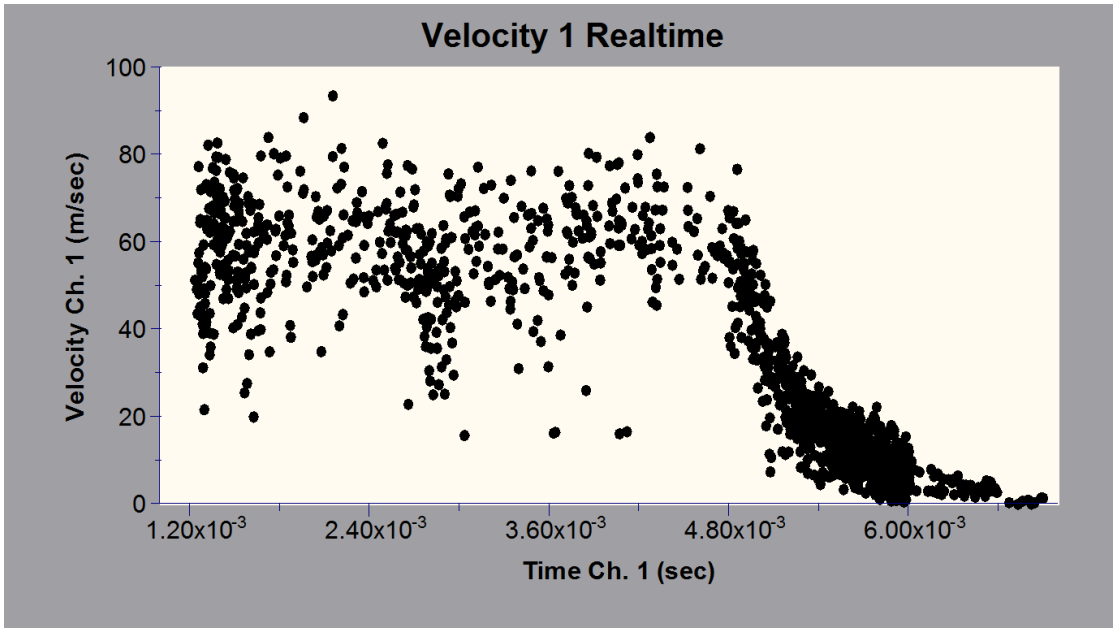

Figure 69: Double injection with 0,2ms interval

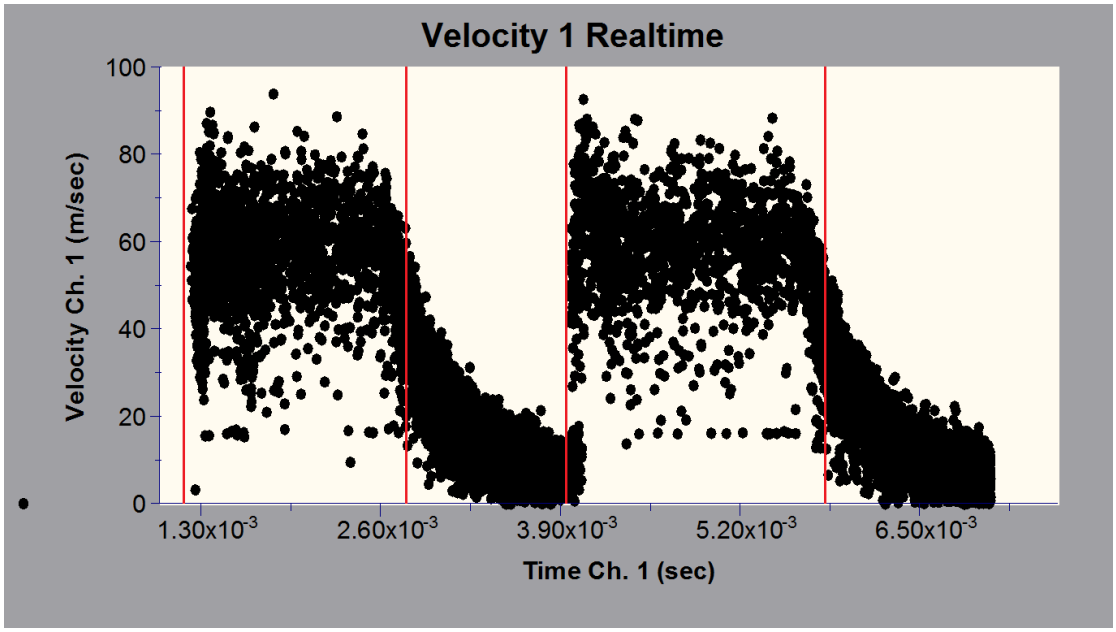

Figure 70: Time-velocity diagram, double injection, 1,0ms interval

The final measurements were performed with a 2ms injection and an 1ms delay between each injection. while the spray core was identified at 27mm radial distance, due to the fact that the conditions were non vaporizing, the average D10 and D32 values vary very little between adjacent positions. Nonetheless at the spray core position the D10 value is 14,5μm and the D32 is 20,5μm for the first injection while the second injection gives a D10 of 14,4μm and a D32 of 19,3μm. The velocities follow the same trend as the droplet diameters, with the average velocity of the first injection reaching 56,1m/s and the second injection reaching 56m/s. The maximum velocity for both injections is about 86m/s.

The variation between the results of the first and second injection can be explained as a first approach with the same explanation that was given for the results of the 5ms injection duration. A pressure wave is created in the fuel rail when the injector opens and if the timing is correct and the pressure wave reaches the injector while is open, a small injection pressure increase is to be expected. For the double injection that will happen during the second injection event, thus leading to somewhat smaller droplets.

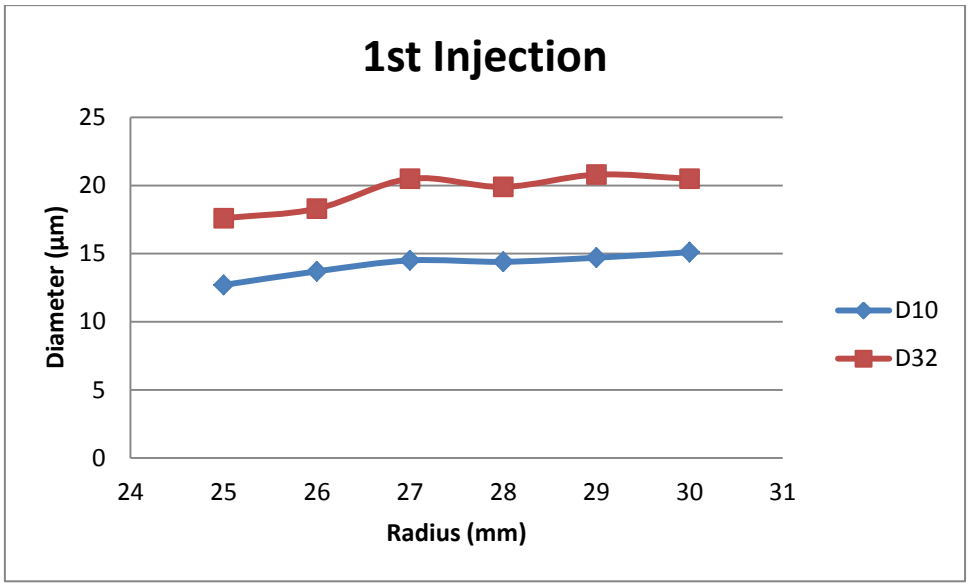

Figure 71: Droplet diameter for six radial positions, first injection

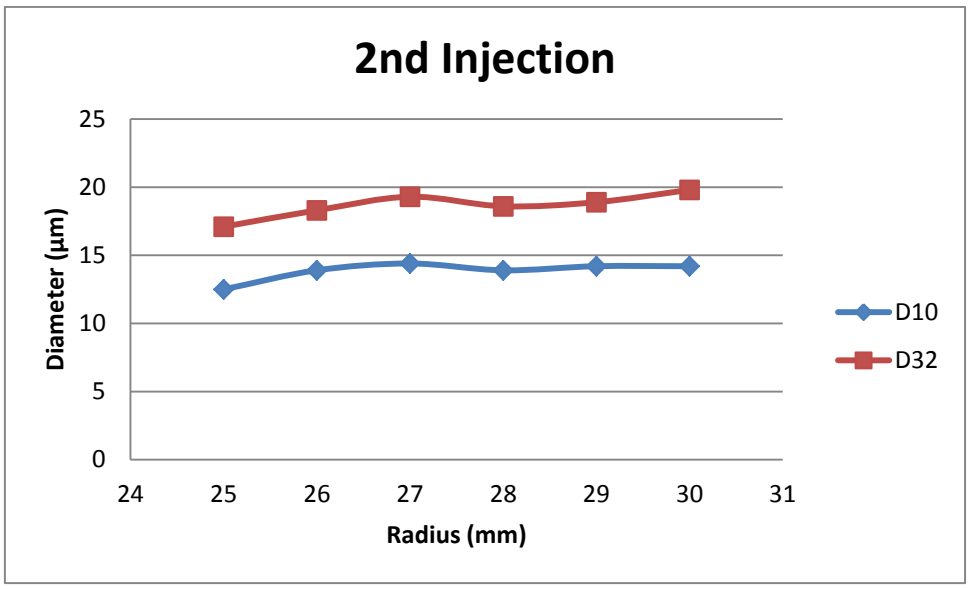

Figure 72: Droplet diameter for six radial positions, second injection

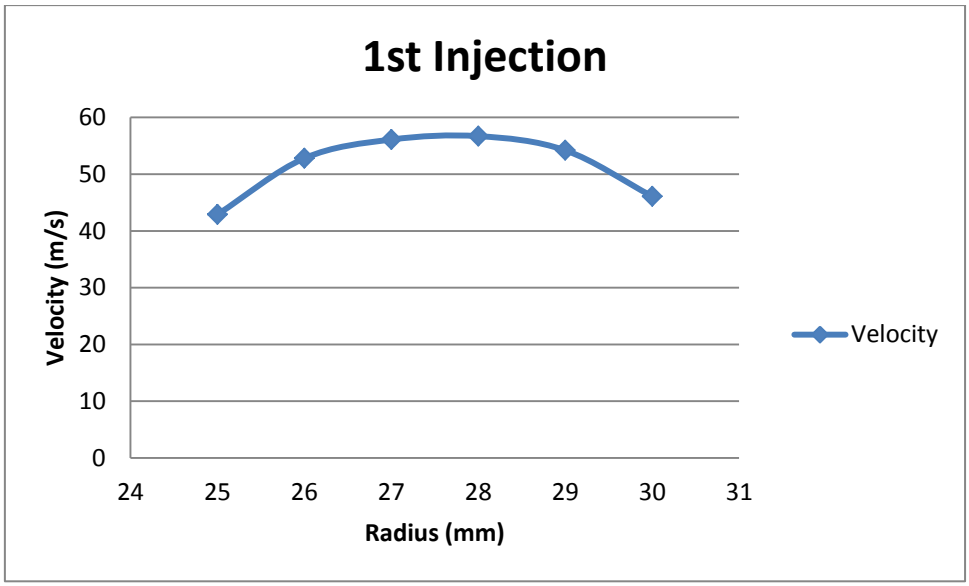

Figure 73: Droplet velocity for six radial positions, first injection

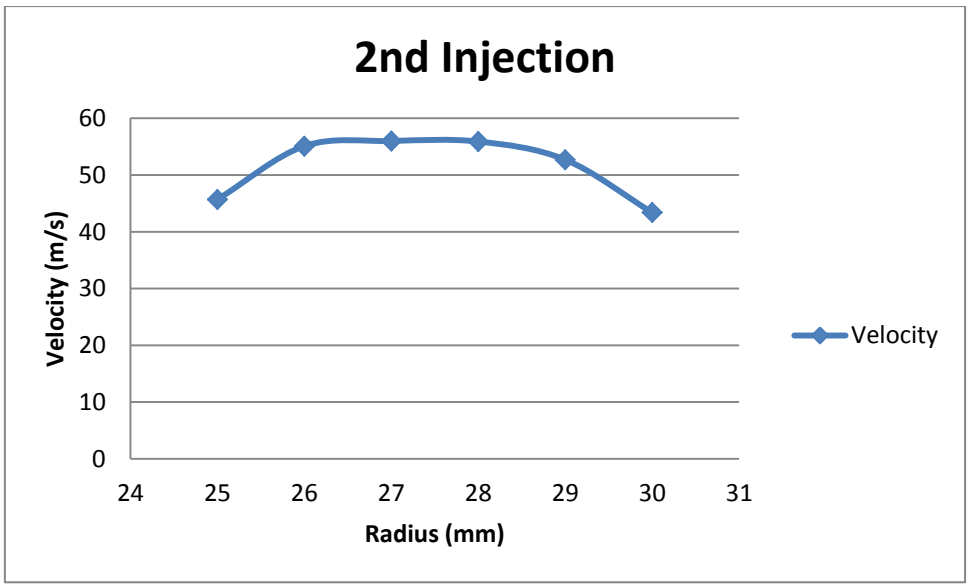

Figure 74: Droplet velocity for six radial positions, second injection

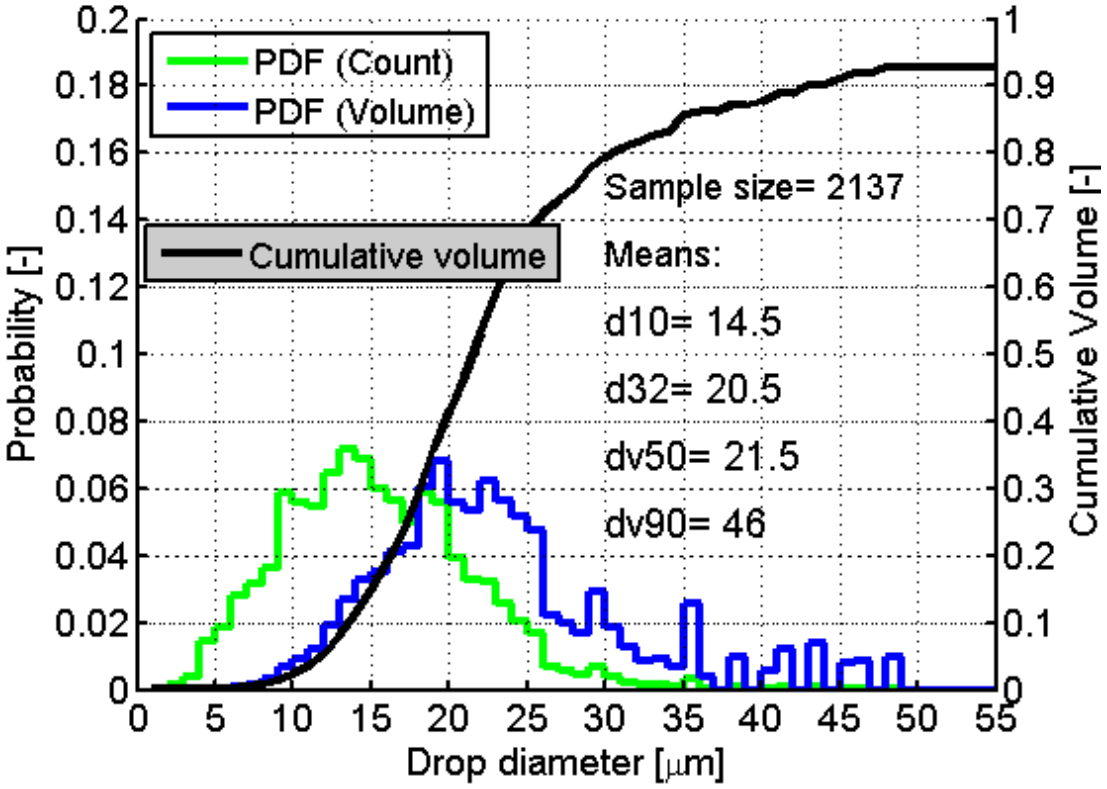

Figure 75: PDF graph and cumulative volume, first injection

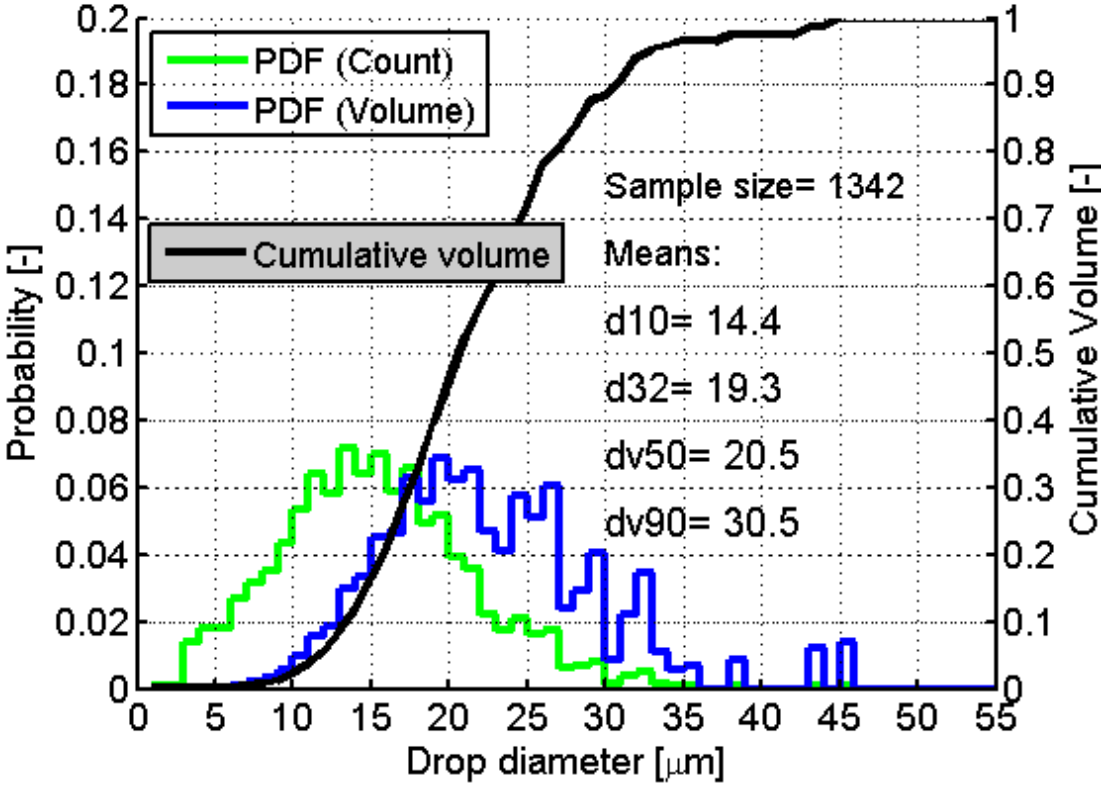

Figure 76: PDF graph and cumulative volume, second injection

5.4.3 Comparison

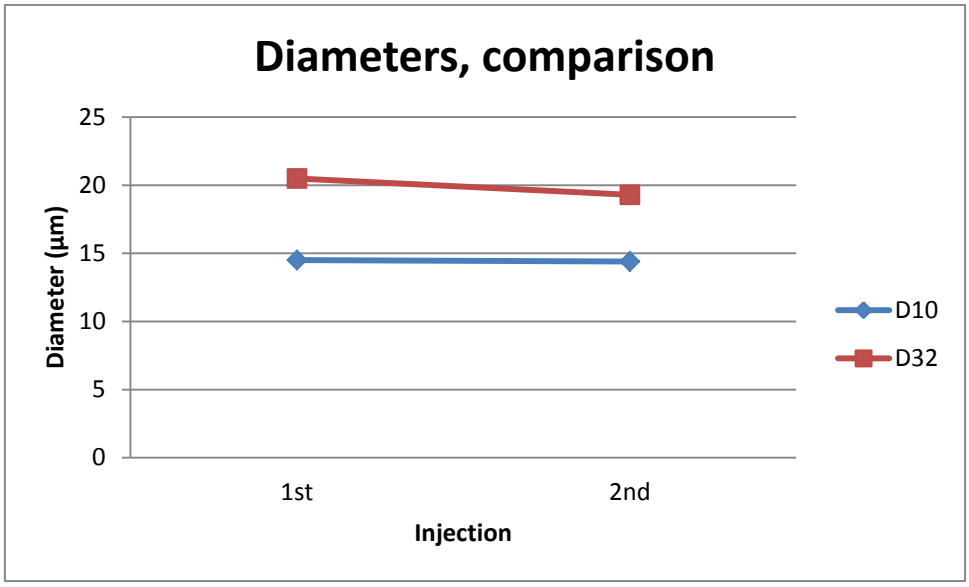

Figure 77: Droplet diameter comparison between first and second injection

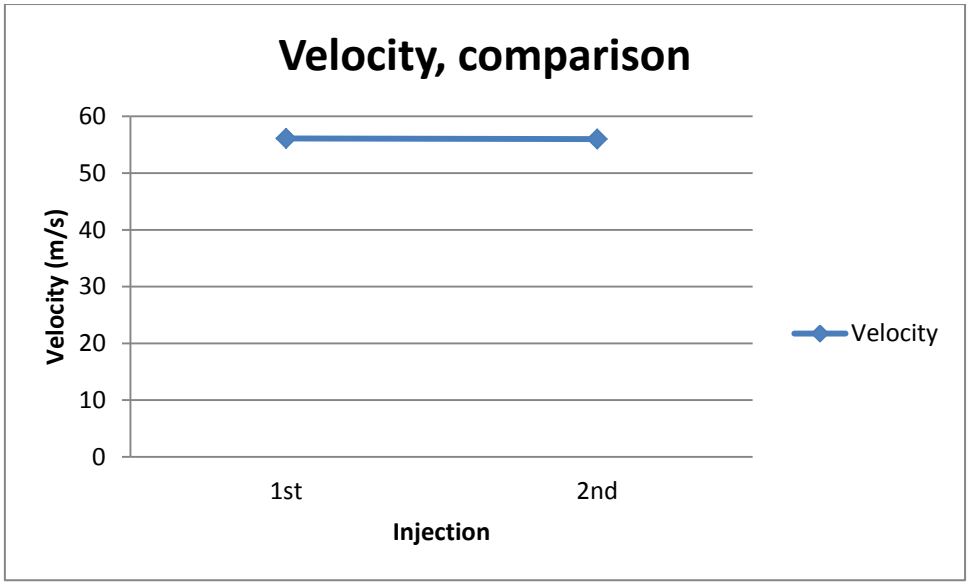

Figure 78: Droplet velocity comparison between first and second injection

6 Conclusion

In the present study an experimental analysis was performed in a new fuel injector in terms of spray characteristics. Both the droplet velocities and droplet diameters were analyzed over a wide range of injection pressures and modes of operation under non vaporizing conditions using Phase Doppler Interferometry (PDI).

From the measurements it is clear that the factor that greatly affects the droplet diameters and the velocity is the injection pressure. As the pressure increases the diameter decreases both in terms of D10 and D32 and seems to reach an asymptote of 11,5μm at pressures of 200bar (D10). The velocity increases as well but after 100bar injection pressure there is a slight decrease, which is attributed to the lower momentum of the small droplets that have higher deceleration due to the surrounding air. For a constant injection pressure, varying the injection duration does not affect the droplet diameters and velocities in any significant way, mainly due to the full opening of the injector needle. Finally the injector is able to perform double injection but again the diameters and the velocities of the droplets do not have significant difference compared to the single injection at the same pressure.

6.1 Further Work

All the previous measurements were conducted in non-vaporizing conditions. The next step would be to test the same injector under the same pressures under vaporizing conditions and with different backpressure levels in order to simulate stratified environment. Furthermore testing of the actual flow rate of the injector for different pressures and injection durations can be performed and afterwards an evaluation of droplet diameters and velocities for the same flow rate but under different injection pressures can be done.

7 Bibliography

Aleiferis, P., & Romunde, Z. v. (2013). An analysis of spray development with iso-octane, n-pentane, gasoline, ethanol and n-butanol from a multi-hole injector under hot fuel conditions. *Fuel , 105*, 143 - 168.

Dahlander, P., & Denbratt, I. (2005). Experimental investigation of fuel pressure influence on droplet size and velocity for a gasoline multi-hole direct injection injector spray under vaporising conditions in a constant pressure chamber. *18th Annual Conference on Liquid Atomization and Spray Systems.* Irvine.

Mayinger, F., & Feldmann, O. (2001). Phase Doppler Anemometry (PDA). In *Optical measurements : techniques and applications* (pp. 139 - 152). Berlin: Springer.

Postrioti, L., Bosi, M., Mariani, A., & Ungaro, C. (2012). *Momentum Flux Spatial Distribution and PDA Analysis of a GDI Spray.* SAE Paper 2012-01-0459.

Skogsberg, M. (2007). *A Study on Spray-Guided Stratified Charge Systems for Gasoline Engines.* Göteborg: Chalmers University of Technology.

Xander, B. (2006). *Grundlegende Untersuchungen an einem Ottomotor mit Direkteinspritzung und strahlgeführtem Brennverfahren.* Universität Karlsruhe.